Novel symmetric bis-benzimidazoles: synthesis, DNA/RNA binding and antitrypanosomal activity

A. Bistrović Popov[a], I. Stolić[b], L. Krstulović[b], M. C. Taylor[c], J. M. Kelly[c], S. Tomić[d], M. Bajić[b], S. Raić-Malić[a*]

[a]*Department of Organic Chemistry, Faculty of Chemical Engineering and Technology, University of Zagreb, Marulićev trg 20, HR-10000 Zagreb, Croatia*

[b]*Department of Chemistry and Biochemistry, Faculty of Veterinary Medicine, University of Zagreb, Heinzelova 55, HR-10000 Zagreb, Croatia*

[c]*Department of Pathogen Molecular Biology, London School of Hygiene and Tropical Medicine, Keppel Street, London, WC1E 7HT, UK*

[d] *Division of Organic Chemistry and Biochemistry, Physical Chemistry, Ruđer Bošković Institute, Bijenička 54, HR-10000 Zagreb, Croatia*

*Corresponding Author:

Tel: 00385-1-4597-213, Fax: 00385-1-4597-224, E-mail: sraic@fkit.hr

Abstract

The novel benzimidazol-2-yl-fur-5-yl-(1,2,3)-triazolyl dimeric series with aliphatic and aromatic central linkers was successfully prepared with the aim of assessing binding affinity to DNA/RNA and antitrypanosomal activity. UV-Visible spectroscopy, thermal denaturation and circular dichroism studies indicated strong and selective interaction of heterocyclic bis-amidines with *ct*DNA and revealed minor groove binding as the dominant binding mode. The amidino fragment and 1,4-bis(oxymethylene)phenyl spacer were the main determinants of activity against *Trypanosoma brucei*. The bis-benzimidazole imidazoline **15c**, which had antitrypanosomal potency in the submicromolar range and DNA interacting properties, emerged as a candidate for further structural optimization to obtain more effective agents to combat trypanosome infections.

Keywords: bis-benzimidazoles, *ct*DNA binding, UV-Vis, CD spectroscopy, thermal denaturation, *Trypanosoma brucei*

1. Introduction

Neglected tropical diseases (NTDs) affect more than 1 billion people, around 15% of the world's population [1]. Human African trypanosomiasis (HAT), or sleeping sickness, is one of the most deadly NTDs, with 65 million people at risk in 36 countries [1–4]. It is caused by two subspecies of the protozoan parasite *Trypanosoma brucei*, which are transmitted to humans through the bite of tsetse flies in sub-Saharan Africa.

Aromatic diamidines have had several applications in antiparasitic therapy, with well-known examples such as berenil and pentamidine [5–7]. Although the bis-benzamidine derivative, pentamidine (Figure 1), has been used clinically against trypanosomiasis for over 70 years [8–10] it is not effective when given orally, can cause severe toxicity, and is unable to kill parasites which have breached the blood-brain barrier during stage 2 HAT [10–12]. A related diamidine, berenil, is not currently used in humans, but it is important for control of animal trypanosomal diseases, which inflict a huge economic burden in sub-Saharan Africa [13]. Additionally, pafuramidine (DB289), which is the oral prodrug of furamidine (DB75) was recently evaluated in phase III clinical trials [14]. Unfortunately, these trials had to be discontinued due to hepatic and renal toxicity [15]. Although aromatic diamidines have been used in the treatment of protozoal diseases for many years, their precise mechanism of action is not fully understood. Various targets have been suggested, including both mitochondrial and nuclear DNA, microtubules, acidocalcisomes, and a range of enzymes [10,12,16–19].

Current therapies for HAT are unsatisfactory and under threat from emerging resistance, what is frequently linked to the activity of transporters responsible for drug uptake [20,21]. This has prompted the search of benzimidazole derivatives that are more efficacious for combating this fatal infection [22–25]. As an example, amidinobenzimidazoles have been developed as potent anti-trypanosomal agents [26–29]. Additionally, it has been shown that introduction of nitrogen atoms into the aromatic system of furamidine changes the lipophilicity and polarity of the heterocyclic core, generating aza analogs that may cross the blood brain barrier (Figure 1) [12,19,21]. Thus, diphenyl furan-based and aza analogs have been developed as candidates for treatment of second-stage HAT. Diamidines containing a 1,2,3-triazole ring as the central core were

the first aromatic members of this class of molecule to show efficacy superior to that of melarsoprol [30].

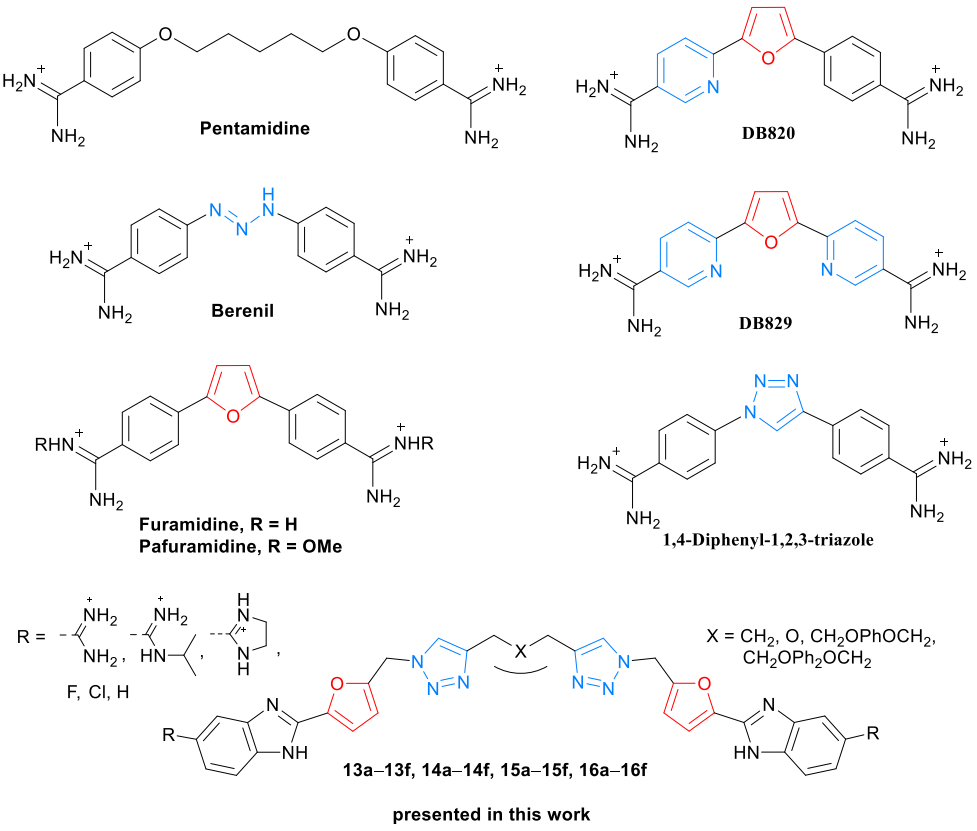

Fig. 1. Structure of compounds with potent antitrypanosomal activities and novel symmetric bis-benzimidazoles **13a**–**13f**, **14a**–**14f**, **15a**–**15f** and **16a**–**16f**.

Based on these studies, and in continuation of our recent work on the development of aromatic amidines as DNA-binding ligands [31,32] and anti-trypanosomal agents [33,34], we aimed here to expand the benzimidazole scaffold to 5-membered furyl and 1,2,3-triazolyl moieties that may adopt helical topology to approximately match the curvature of DNA in the minor groove. Design strategy led to a symmetric series of bis-(benzimidazol-2-yl-fur-5-yl-azole) derivatives connected *via* aliphatic and aromatic linkers (Figure 2). In this context, the influence of diverse linkers and the type of 5-amidine and 5-halogen substituents in bis-benzimidazoles **13a**–**13f**, **14a**–**14f**, **15a**–**15f** and **16a**–**16f** on their DNA/RNA binding affinity and antiprotozoal activity has been explored. Here, we describe the synthesis of novel symmetric bis-benzimidazoles and

their DNA/RNA binding affinities as assessed by UV-Vis and CD spectroscopy, as well as thermal denaturation experiments. Antitrypanosomal potencies of the novel compounds were evaluated and their structure-activity relationship (SAR) is discussed. To better understand the mode of DNA binding, we performed molecular modelling of the most potent trypanocidal compound (**15c**) when bound to the minor groove of DNA.

2. Results and Discussion

2.1. Chemistry

Synthesis of novel symmetric bis-[benzimidazol-2-yl-fur-5-yl-(1,2,3)-triazolyl] derivatives (**13a**–**13f**, **14a**–**14f**, **15a**–**15f** and **16a**–**16f**) was carried out as outlined in Scheme 1. A one-pot route in biphasic mixture HCl-H_3PO_4/$CHCl_3$ was applied for efficient conversion of D-fructose (**1**) to 5-chloromethylfurfural (**2**), as described in literature [35,36], which then in reaction with sodium azide, gave rise to 5-azidomethylfurfural (**3**). The key precursors, symmetric bis-triazolyl aldehydes connected through 1,3-propylene (**8**), oxydimethylene (**9**), 1,4-bis(oxymethylene)phenyl (**10**), 4,4'-bis(oxymethylene)biphenyl (**11**) linkers were synthesized by Cu(I)-catalyzed 1,3-cycloaddition of the azide **3** with corresponding terminal bis-alkynes (**4**–**7**), using microwave irradiation. A click reaction produced bis-(1,2,3-triazolyl) aldehydes **10** and **11** linked through an aromatic spacer, with excellent yield (ca. 98%), while bis-(1,2,3-triazolyl) aldehydes **8** and **9** connected through an aliphatic chain were obtained in lower yield (ca. 36%). Amidino-substituted *o*-phenylenediamines (**12a**–**12c**) were prepared by the Pinner method as previously reported in the literature [37]. Condensation of various *o*-phenylenediamines (**12a**–**12f**) with bis-(1,2,3-triazolyl) aldehydes (**8**–**11**) using $NaHSO_3$ or *p*-benzoquinone, as an oxidative reagent, afforded the target bis-benzimidazole derivatives with 5-amidino- (**13a**–**13c**, **14a**–**14c**, **15a**–**15c** and **16a**–**16c)**, 5-fluoro- (**13d**–**16d**) and 5-chloro-substituted (**13e**–**16e**), as well as non-substituted benzimidazoles (**13f**–**16f**).

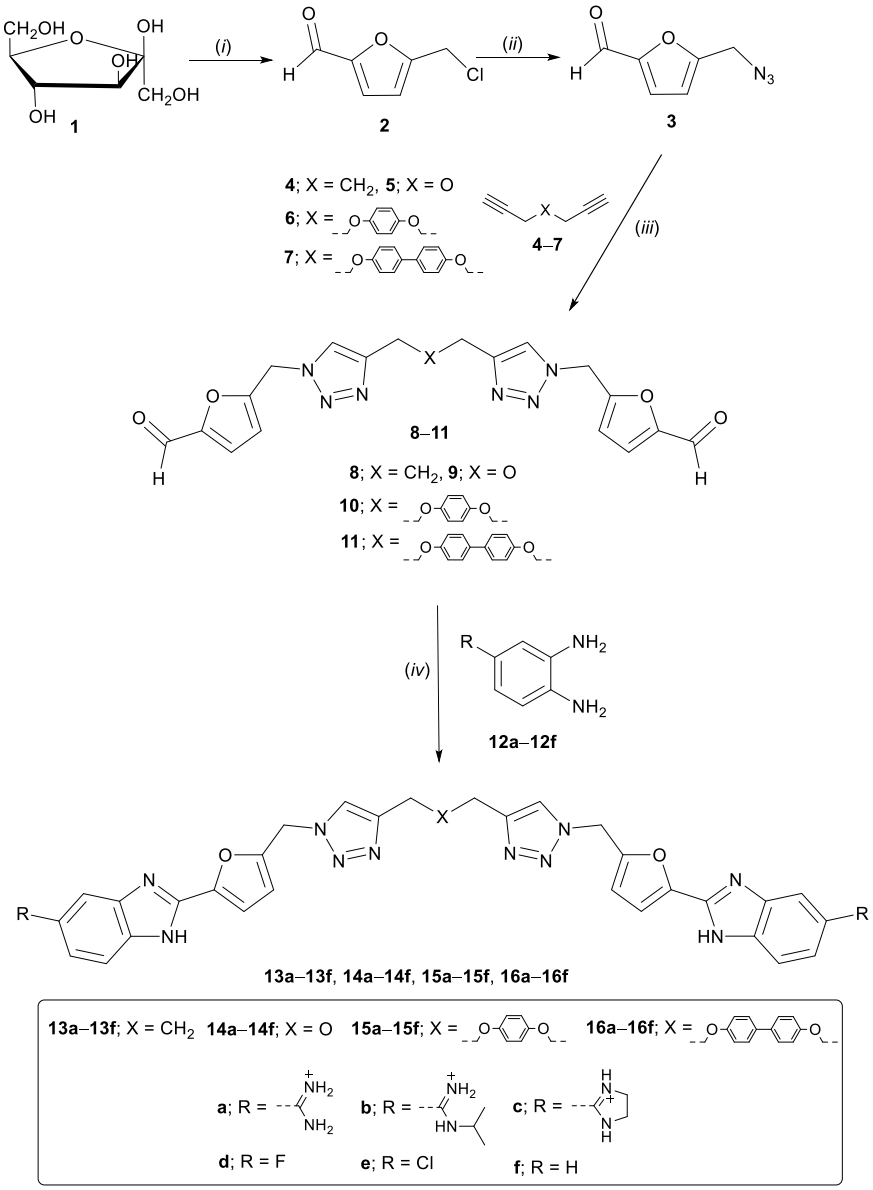

Scheme 1. *Reagents and conditions*: (*i*) HCl: H_3PO_4 = 4: 1, CCl_3, 45 °C, 20 h; (*ii*) NaN_3, AcCN, reflux, 24 h; (*iii*) terminal alkyne, Cu(0), $CuSO_4$, *t*-BuOH: H_2O = 1: 1, DMF, MW, 300 W, 80 °C, 1.5 h; (iv) $NaHSO_3$/*p*-benzoquinone, EtOH, reflux, 6 h.

2.2. Spectroscopic characterization of novel bis-benzimidazoles

The spectroscopic characterization of novel 5-amidino- and 5-halogen-substituted benzimidazoles (**13a**–**13f**, **14a**–**14f**, **15a**–**15f** and **16a**–**16f**) was explored by UV-Vis spectroscopy. Absorption maxima and the corresponding molar extinction coefficients (ε)

are given in Table S1 (Supplementary Information). The changes of the UV-VIS spectra when the temperature was raised to 95 °C were negligible, and the reproducibility of UV-Vis spectra upon cooling back to 25 °C was excellent. Solutions of the studied compounds were stable for many days at room temperature, confirming that all compounds were suitable for further biophysical and biological investigations. The absorbances of compound solutions were proportional to their concentrations between 2 x 10^{-6} and 5 x 10^{-5} moldm^{-3} indicating that they would not aggregate by intermolecular stacking under the experimental conditions used.

2.3. Spectrophotometric titrations of compounds with ds-polynucleotides

UV-Vis absorption measurement is a simple but effective method for detecting complex formation. In general, when a small molecule interacts with DNA/RNA and form a new complex, changes in absorbance and the position of the absorption maxima should occur [38,39]. The interaction of compounds **13a**–**13f**, **14a**–**14f**, **15a**–**15f** and **16a**–**16f** towards *ct*DNA and polyA-polyU were investigated by UV-Vis spectroscopy in a solution of phosphate buffer and DMSO (0.1%). When aliquots of dissolved *ct*DNA were added to the compound solutions, a hypochromic effect (8-45%) was observed, indicating the disappearance of the free molecule and the formation of a new compound-DNA complex (Figure S1, Supplementary Information).

Spectrophotometric titration of compounds **13a**–**13f** and **14a**–**14f,** which contain an aliphatic linker with both polynucleotides, resulted in a pronounced decrease of the absorption maxima at $\lambda > 300$ nm (Table 1, Figure S1, Supplementary Information). Except for **15c**, which interacts with both polynucleotides, other compounds from the **15a**–**15f** series containing a 1,4-bis(oxymethylene)phenyl linker were selective for *ct*DNA. The only exceptions were compounds from the **16a**–**16f** series, which did not display shifts in the UV-Vis absorption maxima. In the UV-Vis spectra of compounds **14b**, **14c**, **13c**, **13f** and **15a**−**15c**, decreases in absorption maxima were followed by bathochromic shifts ($\Delta\lambda$ = 5-10 nm) upon addition of *ct*DNA. Further addition of the *ct*DNA resulted in increased absorption maxima (Figure S1). These results suggested that the above mentioned compounds could form at least two different types of complex. Therefore, binding constants (K_s) were calculated at the $r \geq 0.15$ (r =

[compound]/[*ct*DNA]). At this ratio, changes in absorption maxima were too small for accurate calculation.

To assess the sequence selectivity of the compounds, the experiment was repeated with *ds*-RNA (polyA-polyU) (Figure S1). The addition of polyA-polyU to solutions of compounds containing an aliphatic linker, **13a**–**13f** (with the exception of **13e**) and **14a**–**14f**, induced a hypochromic (10-52%) effect in their UV-Vis spectra. Furthermore, the hypochromic effect was accompanied by a small bathochromic (2-8 nm) shift in the UV-Vis spectra of the unsubstituted amidine and imidazoline derivatives **14a**, **14c**, **13a** and **13c**, as a result of complex formation. Titration of compounds with an aromatic linker, **15a**–**15f** (with the exception of **15c**) and **16a**−**16f**, with polyA-polyU did not show any changes in UV-Vis spectra.

Table 1

Hypochromic effects (H/%)[a], binding constants (logK_s)[b] and ratios n[c] ([compound]/[polynucleotide phosphate]) calculated from the UV-VIS titrations of compounds with *ds*-DNA/RNA (at pH 7, PBS, I = 0.015 M).

Compd	***ct*DNA**			**polyA-polyU**		
	H/%[c]	log *Ks*	*n*	H/%[c]	log *Ks*	*n*
13a	13.3[f]	6.61	0.05	45.9	5.70	0.3[d]
13b	24.0[f]	6.33	0.09	32.3	5.69	0.58
13c	17.0[f]	7.62	0.05	32.1	6.83	0.42
13d	45.8	6.56	0.15[d]	26.6	7.12	0.84
13e	27.2	7.04	0.05[d]	NB	NB	NB
13f	44.6	6.55	0.19	9.9	6.54	0.13[d]
14a	36.6	5.93	0.47	24.4	6.65	0.43[d]
14b	20.5[f]	5.68	0.67	12.9	6.16	0.30[d]
14c	28.1	6.23	0.89	3.4	7.17	0.85[d]
14d	35.4	5.93	0.47	51.2	6.43	0.35
14e	35.3	5.21	0.21	52.2	5.12	0.19
14f	35.8	6.22	0.29	41.1	5.76	0.31
15a	8.7	6.80	0.3[d]	11.3[e]	-	-
15b	23.2[f]	7.31	0.9[d]	41.5[e]	-	-
15c	5.9 [f]	6.05	0.18	10.7	-	-
15d	24.5	5.92	0.17	NB	-	-
15e	26.7	6.33	0.65	NB	-	-
15f	35.2	6.18	0.10	6.0[e]	-	-

[a] Hypochromic effect calculated by Scatchard for compounds;
H = (Abs(compound) –Abs(complex)) / Abs(compound) x 100
[b] Titration data were processed according to the Scatchard equation
[c] Accuracy of n ± 10-30%, consequently logK_s values vary in the same order of magnitude.
[d] n = fix

[e] Hypochromic effect calculated from experimental data: (Abs(compound) –Abs(complex)) / Abs(compound) x 100
– = changes were too small for accurate calculation of binding constants
[f] mixed binding mode, binding constant were calculated in range r ≥ 0.1
NB = no bindng

Overall, the results of spectrophotometric titration of the **13a**–**13f**, **14a**–**14f** and **15a**–**15f** series of compounds showed that they had higher affinity for *ct*DNA than for polyA-polyU. Since compounds **16a**–**16f** did not show affinity for either polynucleotide, it can be concluded that the 4,4'-bis(oxymethylene)biphenyl linker had a detrimental effect on the interaction. Therefore, these compounds were not evaluated in further DNA/RNA binding assays.

2.4. Thermal denaturation experiments

The evaluation of the DNA/RNA melting temperature (T_m) as a result of ligand intercalation or minor grove binding can be used as an indicator of the interaction between compounds and polynucleotides [40–42]. Temperature-dependent DNA denaturation is associated with changes to the absorbance spectrum of the biomolecule as the result of the breakage of hydrogen bonds between base pairs. Accordingly, to assess the binding affinity of synthesized compounds towards DNA/RNA, the *Tm* values of *ct*DNA and polyA-polyU, in the absence and presence of the symmetrical bis-benzimidazoles, were measured (Table 2).

Table 2

ΔT_m values of compounds with ctDNA and polyA-polyU upon addition of compounds at different ratio *r*[a] (PBS, pH = 7).[b]

Compd	*ct*DNA			polyA-polyU		
	0.1	**0.3**	**0.5**	**0.1**	**0.3**	**0.5**
13a	13.56	12.96	13.84	1.51 33.49[c]	0.61 37.3[c]	9.27 27.6[c]
13b	13.77	14.48	14.77	0.90 49.71[c]	0.53 49.71[c]	0.82 44.01[c]
13c	13.48	13.79	19.12	1.58	1.75 18.95[c]	2.70 17.05[c]
13d	0.81	1.28	1.97	0.80	1.27	2.03

13e	2.09	4.06	2.49	-	-	-
13f	2.61	1.16	3.21	0.30	0.30	0.20
14a	9.19	10.43	12.47	2.22	3.47 32.83[c]	3.25 30.67[c]
14b	8.06	9.70	11.07	1.28	2.01	1.61
14c	12.38	12.68	12.54	3.47	4.01 40.8[c]	ND
14d	0.37	0.46	0.13	0.99	0.99 16.17[c]	1.00 27.08[c]
14e	0.73	1.18	2.61	0.99 33.45 [c]	0.58 33.45[c]	0.56 34.57[c]
14f	0.56	0.72	1.11	0.56	0.37 35.49[c]	0.58 33.04[c]
15a	9.53	10.69	12.32	-	-	-
15b	7.98	10.96	12.16	-	-	-
15c	8.17	8.94	ND	2.73	2.21	-
15d	0.51	1.19	3.36	-	-	-
15e	0.72	1.50	2.02	-	-	-
15f	2.82	3.20	2.56	-	-	-

[a] r = [compound]/[polynucleotide]
[b] Error in ΔT_m: ±0.5 °C.
[c] Biphasic melting curve, values for both melting midpoints were given when possible
− = no binding

Generally, the denaturation experiments indicated a higher affinity of the compounds to *ct*DNA than to the polyA-polyU polynucleotide. This was also confirmed with spectrophotometric titrations. Furthermore, amidine derivatives **13a**–**13c**, **14a**–**14c** and **15a**–**15c** showed higher stabilization of *ct*DNA compared to non-amidines **13d**–**13f**, **14d**–**14f** and **15d**–**15f**, confirming the impact of the amidine moiety on DNA/RNA interactions. Thus, a significant binding affinity was found for **13a**–**13c**, **14a**–**14c** and **15a**–**15c**, which showed the highest ΔT_m values (> 9 °C) for *c*tDNA (r = 0.3). Conversely, all compounds showed slight enhancement in thermal stabilities for polyA-polyU. Moreover, while melting transitions in *ct*DNA experiments were typically monophasic, in the polyA-polyU experiments, strong biphasic transitions occurred, with the exception of **14b**, **13f**, **13d** and **15c** (Table 2). This indicates a secondary binding mode, *i.e.* agglomeration of these compounds along the polynucleotide.

2.5. Circular Dichroism (CD) experiments

Circular dichroism (CD) experiments can be used to determine binding and conformational changes of polynucleotides. The peak observed at 275 nm relates to π–π stacking of the DNA bases, and the peak at 245 nm indicates the helicity, which is characteristic of DNA in right-handed B form. The binding mode of achiral small molecules within the chiral DNA/RNA helix can result in an induced CD spectrum (ICD). Compounds that bind into the minor groove of DNA can induce a new peak in the spectrum, arising from the coupling of electronic transition moments of the ligand and DNA bases in an achiral environment [43,44].

The results of CD studies indicated clear changes in the CD spectra for amidine derivatives **13a**–**13c**, **14a**–**14c** and **15a**–**15c** (Figure S2, Supplementary Information); the negative band showed slight hyperchromicity, while the positive band exhibited significant hypochromicity and a bathochromic shift associated with the partial disruption of the polynucleotide helical chirality caused by the binding of a small molecule. Importantly, a strong induced CD signal (ICD) in the range of 300–500 nm appeared. Furthermore, the positive ICD band suggests that the compounds are positioned along the minor groove, identifying this as the dominant binding mode.

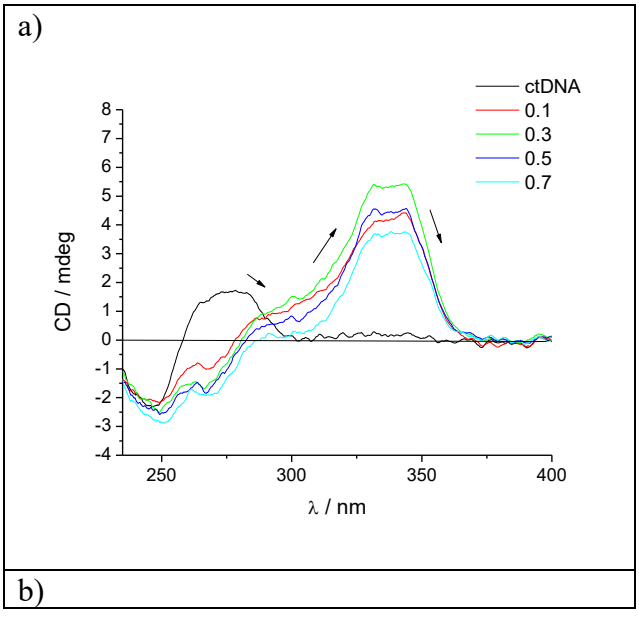

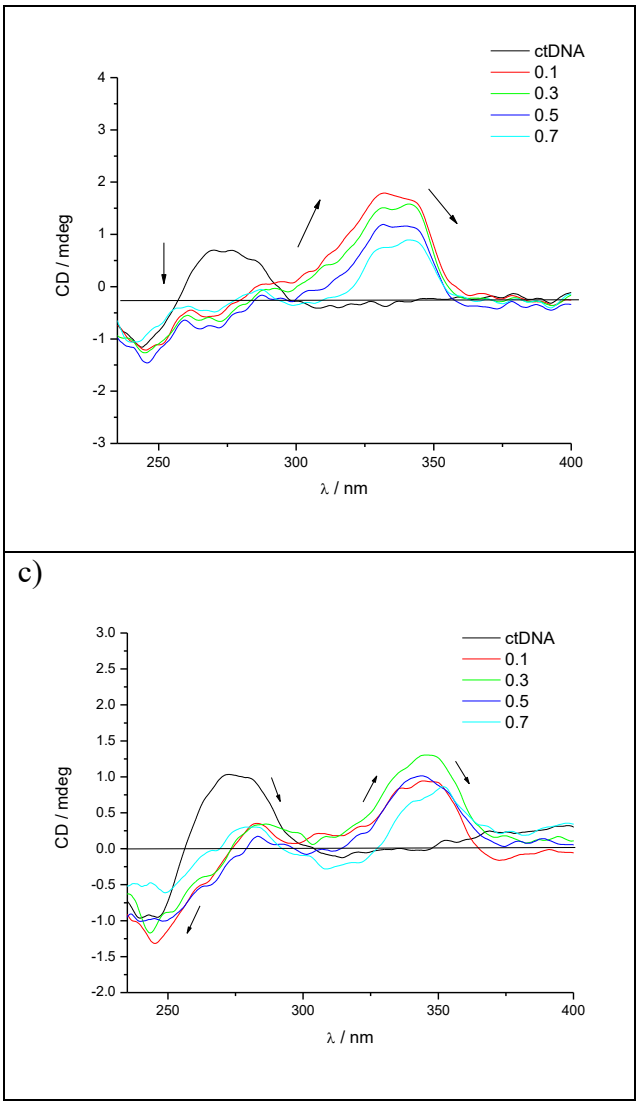

Fig. 2. Induced CD spectra of dimeric compound **15a** (a), compound **15b** (b) and compound **15c** (c) with *ct*DNA (r = 0–0.7).

Conversely, when non-amidine derivatives **13d**–**13f**, **14d**–**14f** and **15d**–**15f** were combined with *ct*DNA, there was little or no perturbation of base stacking, with the helicity bands retaining their basic shape (Figure S2, Supplementary Information).

These findings are in agreement with UV-Vis titrations and denaturation experiments, which also indicated the lower affinity of these compounds compared to amidine derivatives. Most likely, the lack of the amidine groups, which are able to form additional H-bonds with bases, decreases the possibility that stable complexes could

form. The strongly non-linear dependence of the ICD intensity at > 300 nm is in agreement with the calculated values of the UV-Vis titrations and ratios obtained in denaturation experiments. The binding mode of the novel compounds was further investigated by measuring their induced CD in the presence of polyA-polyU. In contrast to *ct*DNA, the addition of polyA-polyU to unsubstituted amidine derivatives (Figure S2, Supplementary Information) resulted in hypochromicity and a bathochromic shift of the CD band at 263 nm. Positive ICD bands appeared at 300 nm, indicating groove binding as the dominant binding mode. Isopropylamidine derivatives showed low affinity for polyA-polyU. Interestingly, the ICD spectra of imidazoline derivatives **13c**, **14c** and **15c** showed a negative signal at > 300 nm, which may indicate intercalation as a possible binding mode. Moreover, minimal changes in CD spectra upon addition of non-amidine compounds to polyA-polyU were observed. This is in agreement with the results on UV-Vis titration and denaturation experiments.

2.6. Screening of the antitrypanosomal activity and structure-activity relationship (SAR)

Results of the *in vitro* testing of novel bis-[benzimidazol-2-yl-fur-5-yl-(1,2,3)-triazolyl] derivatives **13a**–**13f**, **14a**–**14f**, **15a**–**15f** and **16a**–**16f** and nifurtimox, as a reference drug, against bloodstream form *T. brucei* are summarized in Table 3. The cytotoxicity of the most active compounds (IC_{50} < 5 μM) was also assessed using the rat myoblast cell line L6.

Table 3

Antitrypanosomal activity[a] of compounds **13a**–**13f**, **14a**–**14f**, **15a–15f** and **16a–16f** against *Trypanosoma brucei* strain.

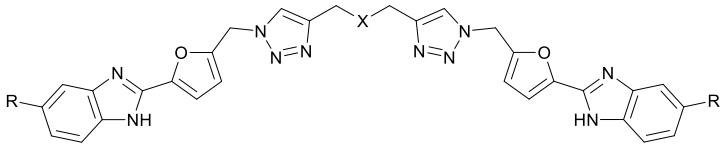

Compd	R	X	*T. brucei*		L6 cells	SI[c]
			IC_{50} /μM	IC_{90} /μM	IC_{50} /μM	
13a		CH_2	3.6 ± 0.4	5.5 ± 0.2	198 ± 3	55
13b		CH_2	5.1 ± 0.2	8.2 ± 1.0	104 ± 3	20

13c		CH_2	3.9 ± 0.3	5.4 ± 0.1	216 ± 21	55
13d	F	CH_2	4.0 ± 0.2	8.9 ± 0.6	221 ± 12	55
13e	Cl	CH_2	3.0 ± 0.3	7.2 ± 0.7	>300	>100
13f	H	CH_2	>15	-	-	-
14a		O	3.3 ± 0.3	4.7 ± 0.1	88.6 ± 2.1	25
14b		O	7.9 ± 0.1	10.8 ± 0.1	-	-
14c		O	3.8 ± 1.0	6.0 ± 0.4	122 ± 3	30
14d	F	O	7.9 ± 0.3	>25	-	-
14e	Cl	O	6.4 ± 0.6	11.8 ± 1.1	-	-
14f	H	O	>15	-	-	-
15a		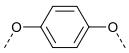	1.3 ± 0.1	5.6 ± 0.4	39.6 ± 2.0	30
15b			1.5 ± 0.1	2.8 ± 0.4	121 ± 5	80
15c		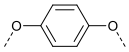	0.75 ± 0.15	1.5 ± 0.1	60.7 ± 3.1	80
15d	F	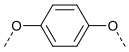	3.4 ± 0.2	6.7 ± 1.0	219 ± 41	65
15e	Cl	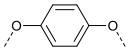	1.4 ± 0.2	2.5 ± 0.4	>270	>190
15f	H		>15	-	-	-
16a		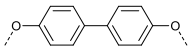	>10	-	-	-
16b		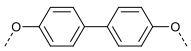	>10	-	-	-
16c		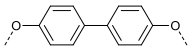	>10	-	-	-
16d	F	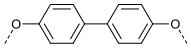	>15	-	-	-
16e	Cl	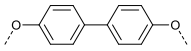	0.37 ± 0.06	9.7 ± 0.03	30.4 ± 6.1	80
16f	H	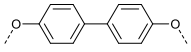	>10	-	-	-
Nifurtimox	-	-	4.4 ± 0.7[b]	-		

[a] *In vitro* activity against bloodstream form of *T. brucei* expressed as the concentration that inhibited growth by 50% (IC_{50}) and 90% (IC_{90}). Data are the mean of triplicate experiments ± SEM.
[b] Taken from ref. [45].
[c] Selectivity index: IC_{50} *Tb*/L6 cells.

The effects of both substituents at the 5-position on the benzimidazole moiety and varied aliphatic and aromatic central linkers were investigated (Figure 3). With the exception of the 5-unsubstituted benzimidazoles **13f**, **14f** and **15f** and the bis-benzimidazoles **16a**–**16d** and **16f**, which have a 1,4-bis(oxymethylene)phenyl linker, all

compounds showed good activity against *T. brucei,* with IC_{50} values ranging from 0.75 μM to 7.9 μM. Among the 5-amidinobenzimidazoles, non-substituted amidines and imidazolines exhibited better potencies than their *N*-isopropyl-substituted counterparts. Similarly, non-substituted amidine **13a**, **15a** and imidazoline **13c**, **15c** benzimidazoles were generally the most active compounds, and were also more potent than nifurtimox. From non-amidine substituted benzimidazoles, antitrypanosomal activities decreased in the following order: Cl > F > H. 5-unsubstituted benzimidazoles **13f**–**16f** had no significant potency against *T. brucei* (IC_{50} > 10 μM), revealing that 5-substitutions in the benzimidazole are crucial for activity. Assessment of the effect of central linkers in the symmetric bis-benzimidazoles on antitrypanosomal potencies, showed that compounds bearing propylene (**13a**–**13f**) and oxydimethylene (**14a**–**14f**) linkers exhibited comparable activities, indicating that the aliphatic spacer was not a determinant of the activity. However, the placement of aromatic linkers did significantly affected potency against *T. brucei*. For example, compounds with 1,4-bis(oxymethylene)phenyl were devoid of activity. The only exception was 5-chlorobenzimidazole **16c**, which exerted a strong inhibitory effect (IC_{50} = 0.37 μM), although its IC_{90} value of 9.7 μM was relatively high compared to the majority of the 5-substituted bis-benzimidazoles. In contrast, the 4,4'-bis(oxymethylene)biphenyl linker increased the trypanocidal activity (IC_{50} = 0.75-3.4 μM) of 5-substituted benzimidazoles **15a**–**15e**. Compound **15c**, which contains both the imidazoline fragment and the 1,4-dimethoxyphenyl spacer had potent activity (IC_{50} = 0.75 μM, IC_{90} = 1.5 μM). The compounds displayed only moderate or negligible cytotoxicity when tested against L6 cells, with selectivity indices ranging from 20 (**13b**) to beyond 270 (**15e**).

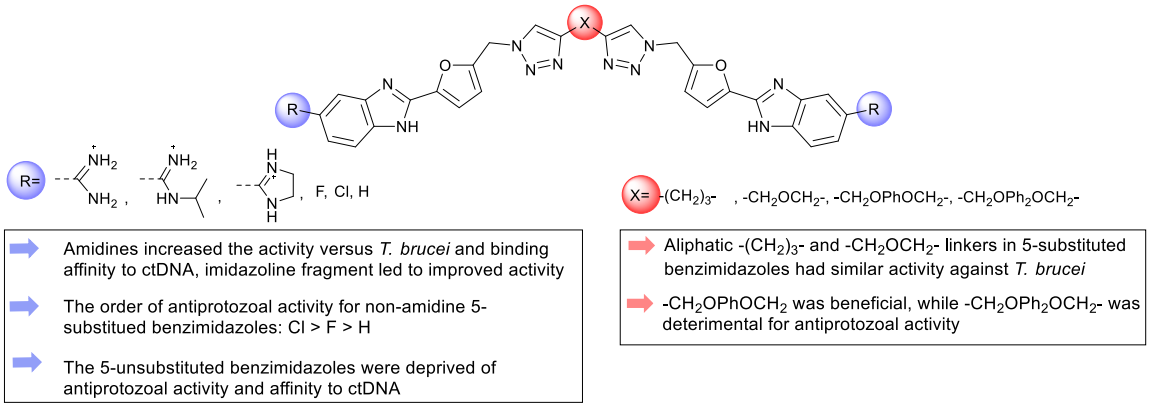

Fig. 3. Structure-activity relationship (SAR) of novel bis-benzimidazoles series with diverse aliphatic and aromatic linkers.

We found a correlation between binding affinities to *ct*DNA and antitrypanosomal activity in the novel bis-benzimidazoles. For example, compounds from the **16a**–**16f** series that were inactive also showed no affinity to the polynucleotides. Similarly, unsubstituted benzimidazoles **13f**–**16f**, which had the lowest affinity for *ct*DNA relative to corresponding analogs, displayed no significant antitrypanosomal potency. In contrast, amidines and imidazolines, which showed the highest and most selective binding affinity to *ct*DNA, also displayed the best activity against *T. brucei*. Structural requirements that were found to influence antitrypanosomal activity and binding affinity to *ct*DNA are presented in Figure 3.

*2.7. Molecular modelling of bis-benzimidazole derivative **15c***

To additionally verify suggested interactions of **15c**, the compound that exhibited the most potent antitrypanocidal activity, binding into the DNA minor groove was further analysed using *in silico* molecular studies. Two B-DNA oligomers with different base pair sequences, the 12 bp DNA d[(CGCGAATTCGCG)]$_2$ (pdb: 1BNA) and 14 bp DNA d[(CTACCGATAAGCAG)]$_2$ (pdb: 5XOG), were used as DNA templates. It was found that compound **15c** fits nicely into the minor groove of both B-DNA models (Figure 4a and 4b). The complex was stabilized with hydrogen bonds and electrostatic interactions with different nucleotide units, phosphate groups, sugars and bases. In the 14 bp DNA-**15c** complex the ligand has interacted with DNA through hydrogen-bonds with phosphate group at A10 and with T8 O2 in one run, and with H-bonds T26 O2, T8 O2

and with phosphate group at C23 in the other run. During MD simulations of the 12 bp DNA-**15c** complex the ligand established hydrogen bonds with phosphate groups at T7, A17 and terminal G12. It should be noted that the shape of the 12-mer DNA after binding of **15c** was preserved during the simulation in accordance with previous results [46,47] (Figure 4c).

Molecular modelling studies revealed that compound **15c** could tightly bind within the *ct*DNA minor groove, whereas **15c** could not bind as efficiently to the much narrower polyA-polyU, as is evident from the thermal denaturation and CD spectroscopy results (Table 2, Figure 2c).

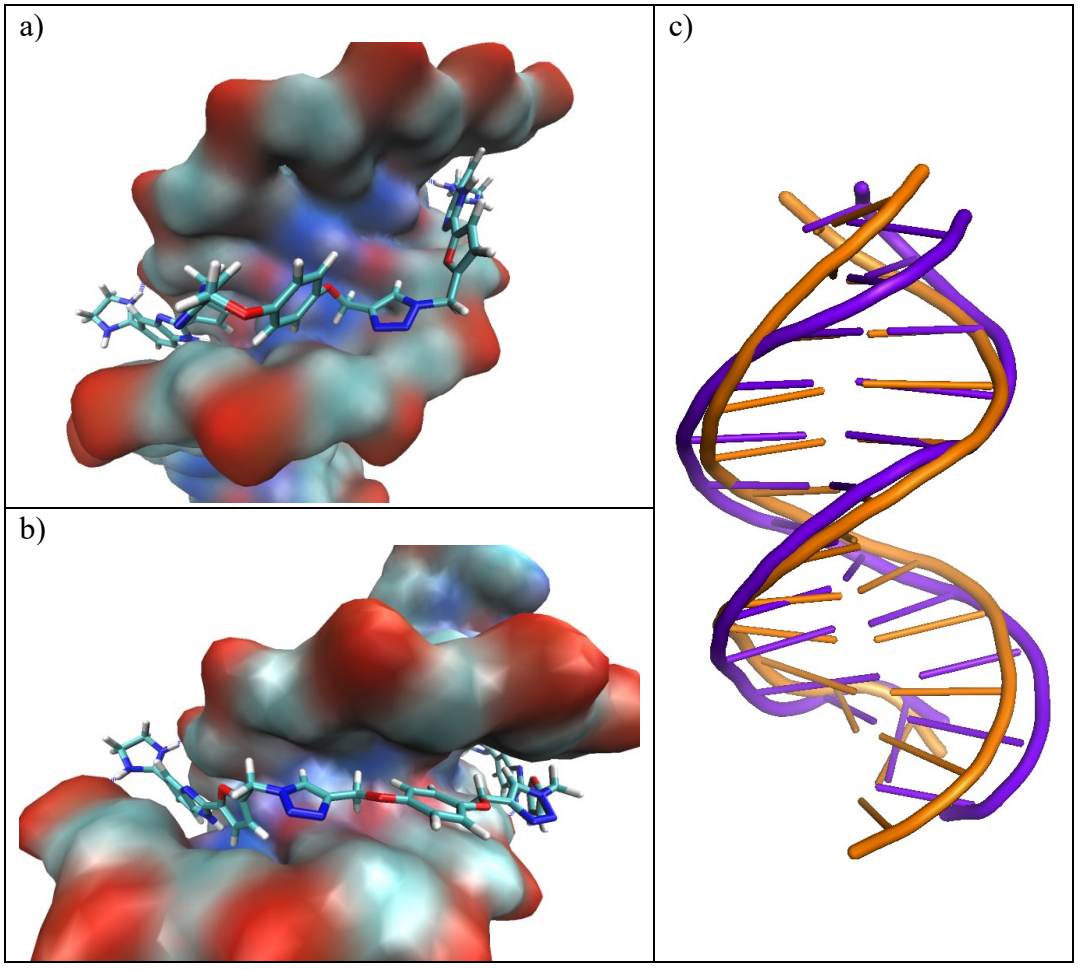

Fig. 4. Complex of **15c** with 14 bp DNA d[(CTACCGATAAGCAG)]$_2$ (a). The ligand is shown in stick representation and the oligonucleotide is represented by its electrostatic potential surface with phosphate group at A10 and with T8 O2 that interact with **15c** through hydrogen bonds (blue dotted line). Compound **15c** bound into the minor groove

of 12 bp DNA d[(CGCGAATTCGCG)]$_2$ (b). The ligand is shown in stick representation and the oligonucleotide is represented by its electrostatic potential surface with phosphate group at T7, A17 and G12 interacting with **15c** through hydrogen bonds (blue dotted line). Aligment of the 12 bp DNA structures before (orange) and after (violet) binding the compound **15c** (c).

3. Conclusions

We report here an efficient pathway for the construction of the dimeric benzimidazole-furan-1,2,3-triazole series **13a**–**13f**, **14a**–**14f**, **15a**–**15f** and **16a**–**16f**. These contain symmetric units connected *via* varied aliphatic and aromatic central linkers. DNA/RNA binding assays showed that bis-5-amidinobenzimidazoles **13a**–**13c**, **14a**–**14c** and **15a**–**15c** had the highest affinity and selectivity for *ct*DNA. The strong interactions with *ct*DNA were supported by spectrophotometric titrations that exhibited a steady decrease in absorbance, accompanied with blue shift. Furthermore, thermal denaturation experiments, which identified ΔT_m values for *ct*DNA above 9 °C, and changes in the CD spectra for bis-5-amidinobenzimidazoles were consistent with non-intercalative and minor-groove binding, as dominant binding mode. Results of antitrypanosomal evaluations showed that bis-5-amidinobenzimidazoles **15a**–**15c**, with a 1,4-bis(oxymethylene)phenyl spacer, exerted the highest activity against *T. brucei*.

Overall, the results revealed that amidino fragments at the 5-position of the benzimidazole ring play a key role in binding affinity to *ct*DNA, while the 5-substituent and linker are crucial determinants of antiprotozoal activity. We found that imidazoline and 1,4-bis(oxymethylene)phenyl were favourable for strong antiprotozoal activity. Bis-benzimidazole imidazoline **15c**, which contains a 1,4-bis(oxymethylene)phenyl, was the most potent derivative with 6-fold higher activity than nifurtimox. Taken together, our results suggest that compound **15c** binds to *ct*DNA *via* a groove binding mode and that this DNA interacting property may be responsible for its antitrypanosomal potency. Moreover, molecular modelling revealed that compound **15c** adopts a concave shape that fits into the minor groove of DNA. The demonstration of DNA binding affinity and

antitrypanosomal potency of this type of compounds, together with their low toxicity against mammalian cells, also suggests that bis-amidinobenzimidazole-furan-azole analogs provide an interesting framework for future structural optimization to obtain promising agents for treatment of human African trypanosomiasis (HAT).

4. Experimental

4.1. General

All solvents were purified using recommended drying agents and/or distilled over 3 Å molecular sieves. For monitoring the progress of a reaction and for comparison purposes, thin layer chromatography (TLC) was performed on pre-coated *Merck* silica gel 60F-254 plates using an appropriate solvent system and the spots were detected under UV light (254 nm). For column chromatography, silica gel (*Fluka*, 0.063-0.2 mm) was employed, and glass columns slurry-packed under gravity. Melting points (uncorrected) were determined with *Kofler* micro hot-stage (*Reichert*, Wien). ^{1}H and ^{13}C NMR spectra were acquired on a *Bruker* 300 and 600 MHz NMR spectrometer, or 300 MHz Agilent Technologies DD2 NMR spectrometer. All data were recorded in DMSO-d_6 at 298 K. Chemical shifts were referenced to the residual solvent signal of DMSO at δ 2.50 ppm for ^{1}H and δ 39.50 ppm for ^{13}C. Individual resonances were assigned on the basis of their chemical shifts, signal intensities, multiplicity of resonances and H–H coupling constants. High performance liquid chromatography was performed on an *Agilent 1100* series system with UV detection (photodiode array detector) using Zorbax C18 reverse-phase analytical column (2.1 x 30 mm, 3.5 µm). All compounds used for biological evaluation showed > 95 % purity in this HPLC system. Microwave-assisted syntheses were performed in a Milestone start S microwave oven using glass cuvettes at 80 °C and 800 W under pressure of 1 bar.

4.2. Experimental procedures for the preparation of compounds

Compound 5-(chloromethyl)furan-2-carbaldehyde (**2**) [36], 1,4-bis(prop-2-yn-1-yloxy)benzene (**6**) [48], 4,4'-bis(prop-2-yn-1-yloxy)-1,1'-biphenyl (**7**) [49], 3,4-diaminobenzimidamide (**12a**) [37], 3,4-diamino-*N*-isopropylbenzimidamide (**12b**) [37],

4-(4,5-dihydro-1*H*-imidazol-2-yl)benzene-1,2-diamine (**12c**) [37] were prepared according to known procedures.

*4.2.1. 5-(Azidomethyl)furan-2-carbaldehyde (**3**).* Compound **2** (634 mg, 4.39 mmol) and NaN_3 (1.14 g, 17.54 mmol) were stirred in acetonitrile (20 mL) under reflux over night. The solvent was evaporated to dryness and the residue was purified by column chromatography (CH_2Cl_2 as eluent) to obtain **3** as yellow oil (640.1 mg, 97%). ^{1}H NMR (300 MHz, DMSO) δ 9.59 (1H, s, CHO), 7.53 (1H, d, *J* = 3.5 Hz, H3'), 6.78 (1H, d, *J* = 3.5 Hz, H4'), 4.63 (2H, s, CH_2). ^{13}C NMR (75 MHz, DMSO) δ 178.50, 156.04, 152.50, 123.89, 112.68, 36.82.

*4.2.2. General procedure for the synthesis of compounds **8–11***

The corresponding terminal alkyne (**4**–**7**) was dissolved in 0.5 mL DMF and *t*-BuOH: H_2O = 1: 1 (2-3 mL). Cu(0) (0.5 eq), 1M CuSO4 (1 eq) and azido-derivative **3** (2.2 eq) were added to the reaction mixture and stirred under microwave irradiation for 1.5 h at 80 °C and 300 W. The solvent was evaporated and the residue was purified by column chromatography using CH_2Cl_2: CH_3OH= 100: 1 as an initial eluent.

*4.2.2.1. 1,3-Bis{[1-(5-formylfuran-2-yl)methylene]-1H-1,2,3-triazole-4-yl}propane (**8**).* Compound **8** was prepared using the above mentioned procedure from 1,6-heptadiin **4** (0.25mL, 2.17 mmol) to obtain **8** as white powder (407.6 mg, 48%, m.p. = 142–144 °C). ^{1}H NMR (300 MHz, DMSO) δ 9.56 (2H, s, CHO), 7.95 (2H, s, H5''), 7.52 (2H, d, *J* = 3.5 Hz, H3'), 6.76 (2H, d, *J* = 3.5 Hz, H4'), 5.74 (2H, s, CH_2), 2.66 (4H, t, *J* = 7.5 Hz, $\underline{CH_2}CH_2\underline{CH_2}$), 1.89 (2H, dd, *J* = 15.0, 7.4 Hz, , $CH_2\underline{CH_2}CH_2$. ^{13}C NMR (75 MHz, DMSO) δ 178.39, 154.90, 152.37, 146.87, 124.04, 122.39, 112.23, 45.67, 28.62, 24.42.

*4.2.2.2. Bis{[1-(5-formylfuran-2-yl)methyl])-1H-1,2,3-triazole-4-yl}dimethylene ether (**9**).* Compound **9** was prepared using the above mentioned procedure from propargyl ether **5** (0.21 mL, 2.05 mmol) to obtain **9** as yellow powder (178.1 mg, 23%, m.p. = 102–105 °C). ^{1}H NMR (600 MHz, DMSO) δ 9.56 (2H, s, CHO), 8.19 (2H, s, H5''), 7.52 (2H, d, *J* = 3.5 Hz, H3'), 6.78 (2H, d, *J* = 3.5 Hz, H4'), 5.79 (4H, s, CH_2), 4.58 (4H, s, CH_2).^{13}C

NMR (75 MHz, DMSO) δ 178.40, 154.65, 152.41, 144.05, 124.48, 123.97, 112.35, 62.63, 45.74.

*4.2.2.3. 1,4-Bis{[(1-((5-formylfuran-2-yl)methylene)-1H-1,2,3-triazole-4 yl]methyleneoxy}benzene (**10**).* Compound **10** was prepared using the above mentioned procedure from **6** (150 mg, 0.81 mmol) to obtain **10** as white powder (386.8 mg, 98%, m.p. = 163–165 °C). ^{1}H NMR (300 MHz, DMSO) δ 9.57 (2H, s, CHO), 8.28 (2H, s, H5''), 7.53 (2H, d, *J* = 3.6 Hz, H3'), 6.96 (4H, s, Ph), 6.80 (2H, d, *J* = 3.5 Hz, H4'), 5.82 (4H, s, CH_2), 5.08 (2H, s, CH_2).^{13}C NMR (75 MHz, DMSO) δ 178.40, 154.59, 152.43, 152.28, 143.29, 124.86, 123.99, 115.60, 112.42, 61.40, 45.78.

*4.2.2.4. 4,4′-Bis{[1-(5-formylfuran-2-yl)methylene)-1H-1,2,3-triazole-4-yl]methyleneoxy}-1,1′-biphenyl (**11**).* Compound **11** was prepared using the above mentioned procedure from **7** (150 mg, 0.57 mmol) to obtain **11** as white powder (311.7 mg, 97%, m.p. = 216–218 °C). ^{1}H NMR (300 MHz, DMSO) δ 9.57 (2H, s, CHO), 8.33 (2H, s, H5''), 7.58–7.51 (6H, m, *J* = 6.0, 5.1 Hz, H3'; Ph), 7.09 (4H, d, *J* = 8.8 Hz, Ph), 6.81 (2H, d, *J* = 3.6 Hz, H4'), 5.83 (4H, s, CH_2), 5.19 (4H, s, CH_2).^{13}C NMR (151 MHz, DMSO) δ 178.39, 157.14, 154.55, 152.44, 143.12, 132.58, 127.24, 124.95, 123.95, 115.10, 112.44, 61.02, 45.80.

4.2.3. *General procedure for the synthesis of compounds **13a–13b, 14a–14c, 15a–15b** and **16a–16e***

The reaction mixture of dimeric bis-triazolylfuraldehyde derivatives (**8**–**11**), *o*-phenylenediamine (**12a**–**12f**) and water solution of $NaHSO_3$ (40%, 1 mL) was dissolved in 15 mL EtOH and stirred under reflux for 6–8 h. After completition of the reaction $NaHSO_3$ was filtered and the reaction mixture was evaporated to dryness. Water was added (5 mL) and the mixture was stirred over night and filtered. The crude residue was dissolved in HCl saturated MeOH (8–10 mL) and stirred over night. Addition of ether resulted in precipitation of products ***13a–13b, 14a–14c, 15a–15b and 16a–16e***.

*4.2.3.1. 1,3-Bis{1-[((5-(5-amidino)benzimidazol-2-yl)furan-2-yl)methylene]-1H-1,2,3-triazole-4-yl}propane hydrochloride (**13a**).* Compound **13a** was prepared using the above

described method from **8** (150 mg, 0.38 mmol) and **12a** (155.8 mg, 0.84 mmol) to obtain **13a** as brown powder (178.2 mg, 55%, m.p. = 197–200 °C). ^{1}H NMR (300 MHz, DMSO) δ 9.34 (2H, s, NH), 9.00 (2H, s, NH), 8.10 (2H, s, H4), 8.03 (2H, s, H5''), 7.75 (2H, d, *J* = 8.5 Hz, H7), 7.68 (2H, dd, *J* = 8.4, 1.3 Hz, H6), 7.40 (2H, d, *J* = 3.4 Hz, H3'), 6.83 (2H, d, *J* = 3.4 Hz, H4'), 5.75 (4H, s, CH_2), 2.68 (4H, t, *J* = 7.4 Hz, CH_2), 1.99–1.87 (2H, m, CH_2).^{13}C NMR (75 MHz, DMSO) δ 165.72, 152.29, 146.93, 142.93, 139.56, 136.52, 123.42, 122.81, 122.40, 115.75, 115.66, 114.72, 112.86, 45.68, 28.61, 24.48. Anal. calcd. for $C_{33}H_{30}N_{14}O_2$ × 4 HCl × 1.1 H_2O (*Mr* = 820.35): C 48.32, H 4.45, N 23.90; found: C 48.14, H 4.79, N 24.02%.

*4.2.3.2. 1,3-Bis{1-[((5-(5-N-isopropylamidino)benzimidazol-2-yl)furan-2-yl)methylene]-1H-1,2,3-triazole-4-yl}propane hydrochloride (**13b**).* Compound **13b** was prepared using the above described method from **8** (100 mg, 0.25 mmol) and **12b** (118.64 mg, 0.56 mmol) to obtain **13b** as brown powder (69.7 mg, 30%, m.p. = 258–261 °C). ^{1}H NMR (300 MHz, DMSO) δ 9.61 (2H, d, *J* = 7.2 Hz, NH), 9.47 (2H, s, NH), 9.10 (2H, s, NH), 8.11 (2H, s, H4), 8.00 (2H, s, H5''), 7.77 (2H, d, *J* = 8.1 Hz, H7), 7.66–7.54 (4H, m, H6; H3'), 6.86 (2H, s, H4'), 5.77 (4H, s, CH_2), 4.19–3.97 (2H, m, CH), 2.67 (4H, t, *J* = 6.5 Hz, CH_2), 1.98–1.87 (2H, m, CH), 1.29 (12H, d, *J* = 5.9 Hz, $\underline{CH_3}CH\underline{CH_3}$).^{13}C NMR (75 MHz, DMSO) δ 162.04, 151.65, 146.82, 144.69, 143.67, 123.60, 123.06, 122.22, 115.78, 114.54, 112.53, 69.67, 45.60, 44.96, 28.52, 24.39, 21.18. Anal. calcd. for $C_{39}H_{42}N_{14}O_2$ × 4 HCl × 0.7 H_2O (*Mr* = 897.31): C 52.20, H 5.32, N 21.85; found: C 52.59, H 5.61, N 21.66%.

*4.2.3.3. 1,3-Bis{1-[((5-(5-imidazolin-2-yl)benzimidazol-2-yl)furan-2-yl)methylene]-1H-1,2,3-triazole-4-yl}propane hydrochloride (**13c**).* Compound **13c** was prepared using the above described method from **8** (150 mg, 0.38 mmol) and **12c** (192.12 mg, 0.84 mmol) to obtain **13c** as light brown powder (163.0 mg, 48%, m.p. > 250 °C). ^{1}H NMR (300 MHz, DMSO) δ 10.80 (4H, s, NH), 8.39 (2H, s, H5''), 8.09 (2H, s, H4), 7.94 (2H, dd, *J* = 8.6, 1.4 Hz, H6), 7.79 (2H, d, *J* = 8.5 Hz, H7), 7.57 (2H, d, *J* = 3.5 Hz, H3'), 6.86 (2H, d, *J* = 3.4 Hz, H4'), 5.77 (4H, s, CH_2), 4.01 (8H, s, $\underline{CH_2CH_2}$), 2.68 (4H, t, *J* = 7.5 Hz, CH_2), 1.95 (2H, dt, *J* = 14.6, 7.3 Hz, CH_2).^{13}C NMR (75 MHz, DMSO) δ 165.49, 152.43, 147.36, 145.73, 144.03, 141.29, 138.03, 123.90, 122.80, 117.05, 116.88, 115.53, 113.16, 46.17,

44.72, 29.04, 24.93. Anal. calcd. for $C_{37}H_{34}N_{14}O_2 \times 4$ HCl $\times$ 1.9 H_2O (*Mr* = 858.02): C 51.79, H 4.53, N 22.85; found: C 51.96, H 4.74, N 22.63%.

*4.2.3.4. Bis{1-[((5-(5-amidino)benzimidazol-2-yl)furan-2-yl)methylene]-1H-1,2,3-triazole-4-yl}dimethylene ether hydrochloride (**14a**).* Compound **14a** was prepared using the above described method from **9** (150 mg, 0.38 mmol) and **12a** (141.8 mg, 0.84 mmol) to obtain **14a** as brown solid (69.4 mg, 22%, m.p. > 205 °C). ^{1}H NMR (600 MHz, DMSO) δ 9.38 (4H, s, NH), 9.09 (4H, s, NH), 8.29 (2H, s, H5''), 8.12 (2H, s, H4), 7.75 (2H, d, *J* = 8.3 Hz, H7), 7.70 (2H, d, *J* = 8.4 Hz, H6), 7.46 (2H, d, *J* = 3.1 Hz, H3'), 6.86 (2H, d, *J* = 3.3 Hz, H4'), 5.81 (4H, s, CH_2), 4.59 (4H, s, CH_2).^{13}C NMR (75 MHz, DMSO) δ 165.90, 151.31, 145.36, 144.33, 144.10, 124.33, 122.65, 121.98, 114.04, 112.73, 62.69, 45.77. Anal. calcd. for $C_{32}H_{28}N_{14}O_3 \times 4$ HCl $\times$ 0.5 H_2O (*Mr* = 811.51): C 47.36, H 4.10, N 24.16; found: C 47.59, H 3.87, N 24.19%. A232

4.2.3.5. *Bis{1-[((5-(5-N-isopropylamidino)benzimidazol-2-yl)furan-2-yl)methylene]-1H-1,2,3-triazole-4-yl}dimethylene ether hydrochloride (**14b**).* Compound **14b** was prepared using the above described method from **9** (150 mg, 0.38 mmol) and **12b** (168.82 mg, 0.84 mmol) to obtain **14b** as grey powder (134.2 mg, 54%, m.p. = 217–221 °C). ^{1}H NMR (600 MHz, DMSO) δ 9.56 (2H, d, *J* = 7.2 Hz, NH), 9.43 (2H, s, NH), 9.09 (2H, s, NH), 8.32 (2H s, H5''), 8.00 (2H, s, H4), 7.73 (2H, d, *J* = 8.4 Hz, H7), 7.59 (2H, dd, *J* = 8.6, 1.1 Hz, H6), 7.50 (2H, d, *J* = 3.1 Hz, H3'), 6.85 (2H, d, *J* = 3.3 Hz, H4'), 5.81 (4H, s, CH_2), 4.60 (4H, s, CH_2), 4.18–4.11 (2H, m, CH), 1.30 (6H, d, *J* = 6.3 Hz, $\underline{CH_3}CH\underline{CH_3}$).^{13}C NMR (151 MHz, DMSO) δ 162.16, 151.28, 145.03, 144.26, 144.08, 134.06, 124.38, 123.42, 122.89, 114.11, 112.62, 62.67, 45.74, 45.02, 21.27. Anal. calcd. for $C_{38}H_{40}N_{14}O_3 \times 4$ HCl $\times$ 0.2 H_2O (*Mr* = 820.18): C 55.65, H 5.92, N 23.91; found: C 55.34, H 6.15, N 24.06%.

*4.2.3.6. 1,4-Bis{[1-(((5-(5-amidino)benzimidazol-2-yl)furan-2-yl)methylene)-1H-1,2,3-triazole-4-yl]methyleneoxy}benzene hydrochloride (**15a**).* Compound **15a** was prepared using the above described method from **10** (100 mg, 0.20 mmol) and **12a** (83.99 mg, 0.45 mmol) to obtain **15a** as white powder (158.2 mg, 87%, m.p. = 261–263 °C). ^{1}H NMR (600 MHz, DMSO) δ 9.41 (4H, s, NH), 9.12 (4H, s, NH), 8.39 (2H, s, H5''), 8.14 (2H. s, H4), 7.79 (2H, d, *J* = 8.4 Hz, H7), 7.73 (2H, d, *J* = 8.3 Hz, H6), 7.54 (2H, d, *J* = 2.7 Hz,

H3'), 6.95 (4H, s, Ph), 6.90 (2H, d, *J* = 3.0 Hz, H4'), 5.85 (4H, s, CH_2), 5.06 (4H s, CH_2).^{13}C NMR (75 MHz, DMSO) δ 165.82, 152.30, 151.61, 143.78, 143.35, 124.77, 123.01, 122.38, 115.99, 115.58, 114.78, 112.93, 61.41, 45.82. Anal. calcd. for $C_{38}H_{32}N_{14}O_4 \times 4$ HCl × 0.9 H_2O (*Mr* = 910.82): C 50.11, H 4.18, N 22.11; found: C 49.81, H 4.22, N 22.03%.

*4.2.3.7. 1,4-Bis{[1-(((5-(5-N-isopropylamidino)benzimidazol-2-yl)furan-2-yl)methylene)-1H-1,2,3-triazole-4-yl]methyleneoxy}benzene hydrochloride (**15b**).* Compound **15b** was prepared using the above described method from **10** (100 mg, 0.20 mmol) and **12b** (76.33 mg, 0.45 mmol) to obtain **15b** as white powder (121.7 mg, 61%, m.p. = 234–236 °C). ^{1}H NMR (600 MHz, DMSO) δ 9.59 (2H, d, *J* = 7.9 Hz, NH), 9.46 (2H, s, NH), 9.08 (2H, s, NH), 8.41 (2H, s, H5''), 8.01 (2H, s, H4), 7.78 (2H, d, *J* = 8.5 Hz, H7), 7.61 (2H, dd, *J* = 8.5, 1.1 Hz, H6), 7.57 (2H, d, *J* = 3.1 Hz, H3'), 6.96 (4H, s, Ph), 6.90 (2H, d, *J* = 3.3 Hz, H4'), 5.85 (4H, s, CH_2), 5.07 (4H, s, CH_2), 4.10 (2H, td, *J* = 13.0, 6.4 Hz, CH), 1.30 (12H, d, *J* = 6.4 Hz, $\underline{CH_3}CH\underline{CH_3}$).^{13}C NMR (75 MHz, DMSO) δ 162.16, 152.32, 151.59, 144.76, 143.82, 143.35, 124.81, 123.82, 123.26, 115.94, 115.61, 114.72, 112.93, 111.30, 61.43, 45.83, 45.09, 21.30. Anal. calcd. for $C_{44}H_{44}N_{14}O_4 \times 4$ HCl × 1.2 H_2O (*Mr* = 1000.38): C 52.83, H 5.08, N 19.60; found: C 53.05, H 5.07, N 19.47%.

*4.2.3.8. 1,4-Bis{[1-(((5-(5-imidazolin-2-yl)benzimidazol-2-yl)furan-2-yl)methylene)-1H-1,2,3-triazole-4-yl]methyleneoxy}benzene hydrochloride (**15c**).* Compound **15c** was prepared using the above described method from **10** (100 mg, 0.20 mmol) and **12c** (103.02 mg, 0.45 mmol) to obtain **15c** as brown crystals (93.6 mg, 47%, m.p. >250 °C). ^{1}H NMR (300 MHz, DMSO) δ 10.61 (4H, s, NH), 8.35 (2H, s, H5''), 8.31 (2H, s, H4), 7.84 (2H, d, *J* = 8.5 Hz, H7), 7.77 (2H, d, *J* = 8.0 Hz, H6), 7.40 (2H, d, *J* = 3.2 Hz, H3'), 6.95 (4H, s, Ph), 6.86 (2H, d, *J* = 3.4 Hz, H4'), 5.83 (4H, s, CH_2), 5.06 (4H, s, CH_2), 4.01 (8H, s, $\underline{CH_2CH_2}$).^{13}C NMR (75 MHz, DMSO) δ 165.31, 152.29, 150.95, 146.19, 144.99, 143.31, 124.65, 122.65, 115.61, 115.56, 113.43, 112.72, 61.41, 45.83, 44.22. Anal. calcd. for $C_{42}H_{36}N_{14}O_4 \times 4$ HCl × 2.8 H_2O (*Mr* = 997.12): C 50.59, H 4.61, N 19.66; found: C 50.82, H 4.43, N 19.75%.

*4.2.3.9. 4,4′-Bis{[1-(((5-(5-amidino)benzimidazol-2-yl)furan-2-yl)methylene)-1H-1,2,3-triazole-4-yl]methyleneoxy}-1,1'-biphenyl hydrochloride (**16a**).* Compound **16a** was prepared using the above described method from **11** (150 mg, 0.27 mmol) and **12a** (108.25 mg, 0.58 mmol) to obtain **16a** as white powder (181.7 mg, 31%, m.p. = 260–263 °C). ^{1}H NMR (600 MHz, DMSO) δ 9.40 (4H, s, NH), 9.11 (4H, s, NH), 8.43 (2H, s, H5''), 8.14 (2H, s, H4), 7.78 (2H, d, *J* = 8.5 Hz, H7), 7.72 (2H, d, *J* = 8.5 Hz, H6), 7.54–7.48 (6H, m, Ph; H3'), 7.08 (4H, d, *J* = 8.6 Hz, Ph), 6.90 (2H, d, *J* = 3.2 Hz, H4'), 5.86 (4H, s, CH_2), 5.19 (4H, s, CH_2).^{13}C NMR (75 MHz, DMSO) δ 165.86, 157.14, 151.42, 144.11, 143.18, 132.54, 127.23, 124.89, 122.84, 122.20, 115.10, 114.39, 112.91, 61.04, 45.84. Anal. calcd. for $C_{44}H_{36}N_{14}O_4 \times 4$ HCl × 1.5 H_2O (*Mr* = 997.73): C 52.97, H 4.34, N 19.65; found: C 53.18, H 4.22, N 19.97%.

*4.2.3.10. 4,4′-Bis{[1-(((5-(5-N-isopropylamidino)benzimidazol-2-yl)furan-2-yl)methylene)-1H-1,2,3-triazole-4-yl]methyleneoxy}-1,1'-biphenyl hydrochloride (**16b**).* Compound **16b** was prepared using the above described method from **11** (70 mg, 0.12 mmol) and **12b** (46.19 mg, 0.25 mmol) to obtain **16b** as light brown powder (36.3 mg, 28%, m.p. = 236–238 °C). ^{1}H NMR (600 MHz, DMSO) δ 9.56 (2H, d, *J* = 7.6 Hz, NH), 9.42 (2H, s, NH), 9.02 (2H, s, NH), 8.43 (2H, s, H5''), 7.99 (2H, s, H4), 7.76 (2H, d, *J* = 8.4 Hz, H7), 7.59 (2H, d, *J* = 8.3 Hz, H6), 7.51 (4H, d, *J* = 8.6 Hz, Ph), 7.48 (2H, d, *J* = 3.1 Hz, H3'), 7.08 (4H, d, *J* = 8.6 Hz, Ph), 6.89 (2H, d, *J* = 3.2 Hz, H4'), 5.85 (4H, s, CH_2), 5.19 (4H, s, CH_2), 4.08 (2H, dt, *J* = 20.9, 6.7 Hz, H), 1.30 (12H, d, *J* = 6.3 Hz, $\underline{CH_3}CH\underline{CH_3}$).^{13}C NMR (75 MHz, DMSO) δ 162.42, 157.24, 151.24, 145.35, 144.57, 143.26, 132.65, 127.34, 124.95, 123.53, 122.94, 116.23, 115.20, 114.90, 113.87, 112.96, 61.11, 45.93, 45.14, 21.35. Anal. calcd. for $C_{50}H_{48}N_{14}O_4 \times 4$ HCl × 1.6 H_2O (*Mr* = 1083.69): C 55.42, H 5.13, N 18.09; found: C 55.62, H 4.39, N 17.72%.

*4.2.4. General procedure for the synthesis of compounds **14c** and **16c***

The reaction mixture of dimeric bis-triazolylfuraldehyde derivatives (**9**, **11**), *o*-phenylenediamine **12c** (2eq) and *p*-benzoquinone (2 eq) was dissolved in 15 mL EtOH and stirred under reflux for 6–8 h. The reaction mixture was cooled at room temperature, diethyl ether was added, and the resulting solid was filtered off.

*4.2.4.1. Bis{1-[((5-(5-imidazolin-2-yl)benzimidazol-2-yl)furan-2-yl)methylene]-1H-1,2,3-triazole-4-yl}dimethylene ether hydrochloride (**14c**).* Compound **14c** was prepared using the above described method from **9** (100 mg, 0.25 mmol) and **12c** (115.41 mg, 0.50 mmol) to obtain **14c** as brown powder (57.9 mg, 26%, m.p. > 250 °C). ^{1}H NMR (300 MHz, DMSO) δ 10.64 (2H, bs, NH), 8.39–8.22 (4H, m, H4; H5''), 7.88–7.70 (4H, m, H7; H6), 7.39 (2H, d, *J* = 2.0 Hz, H3'), 6.84 (2H, d, *J* = 3.4 Hz, H4'), 5.80 (4H, s, CH_2), 4.59 (4H. s, CH_2), 4.01 (8H, s, $\underline{CH_2CH_2}$).^{13}C NMR (75 MHz, DMSO) δ 165.57, 151.16, 146.40, 145.03, 144.27, 124.47, 122.80, 115.81, 113.57, 112.86, 62.84, 45.94, 44.43. Anal. calcd. for $C_{36}H_{32}N_{14}O_3 \times 4$ HCl × 2.7 H_2O (*Mr* = 903.23): C 47.87, H 4.62, N 21.11; found: C 48.78, H 4.56, N 21.10%.

*4.2.4.2. 4,4′-Bis{[1-(((5-(5-imidazolin-2-yl)benzimidazol-2-yl)furan-2-yl)methylene)-1H-1,2,3-triazole-4-yl]methyleneoxy}-1,1'-biphenyl hydrochloride (**16c**).* Compound **16c** was prepared using the above described method from **11** (150 mg, 0.26 mmol) and **12c** (133.69 mg, 0.58 mmol) to obtain **16c** as white powder (79.1 mg, 29%, m.p. = 246–248 °C). ^{1}H NMR (300 MHz, DMSO) δ 10.71 (4H, s, NH), 8.44 (2H, s, H5''), 8.36 (2H, s, H4), 7.90 (2H, d, *J* = 8.0 Hz, H7), 7.80 (2H, d, *J* = 8.4 Hz, H6), 7.53–7.43 (6H, m, Ph; H3'), 7.07 (4H, d, *J* = 8.4 Hz, Ph), 6.89 (2H, d, *J* = 2.8 Hz, H4'), 5.86 (4H, s, CH_2), 5.18 (4H, s, CH_2), 4.01 (8H, s, $\underline{CH_2CH_2}$). ^{13}C NMR (75 MHz, DMSO) δ 165.18, 157.08, 151.17, 144.47, 143.13, 132.49, 127.15, 124.79, 122.93, 116.80, 115.89, 115.59, 115.07, 114.01, 112.76, 61.02, 45.82, 44.20. Anal. calcd. for $C_{48}H_{40}N_{14}O_4 \times 4$ HCl × 1.4 H_2O (*Mr* = 1048.00): C 55.01, H 4.50, N 18.71; found: C 54.87, H 4.67, N 18.54%.

*4.2.5. General procedure for the synthesis of compounds **13d–13f, 14d–14f, 15d–15f and 16d–16f***

The reaction mixture of dimeric bis-triazolylfuraldehyde derivatives (**8–11**), *o*-phenylenediamine (**12d**, **12e**, **12f**) and 40 % $NaHSO_3$ was dissolved in 15 mL EtOH and stirred under reflux for 6–8 h. After completition of the reaction $NaHSO_3$ was filtered and the reaction mixture was evaporated to dryness. Water was added (5 mL) and the mixture was stirred over night and filtered. The crude residue was dissolved in acetone addition of water resulted in precipitation of products ***13d–13f, 14d–14f, 15d–15f and 16d–16f***.

*4.2.5.1. 1,3-Bis{1-[(5-(5-fluorobenzimidazol-2-yl)furan-2-yl)methylene]-1H-1,2,3-triazol-4-yl}propane (**13d**).* Compound **13d** was prepared using the above described method from **8** (150 mg, 0.38 mmol) and **12d** (105.95 mg, 0.84 mmol) to obtain **13d** as brown powder (161.4 mg, 70%, m.p. = 146–149 °C). ^{1}H NMR (600 MHz, DMSO) δ 13.05 (2H, bs, NH), 7.96 (2H, s, H5''), 7.64–7.21 (4H, m, H4; H7), 7.18 (2H, s, H3'), 7.06 (2H, s, H6), 6.77 (2H, d, *J* = 2.5 Hz, H4'), 5.72 (4H, s, CH_2), 2.67 (4H, t, *J* = 7.3 Hz, CH_2), 1.95–1.89 (2H, m, CH_2). ^{13}C NMR (75 MHz, DMSO) δ 160.32; 157.20 (d, J_{CF} = 235.8 Hz), 150.34, 146.92, 145.51, 144.36, 142.74, 127.74, 122.02, 112.32, 111.60, 110.67; 110.31 (, J_{CF} = 27.0 Hz), 45.71, 28.70, 24.52. Anal. calcd. for $C_{31}H_{24}N_{10}F_2O_2$ × 3.2 H_2O (*Mr* = 664.24): C 56.05, H 4.61, N 21.09; found: C 56.17, H 4.73, N 21.21%.

*4.2.5.2. 1,3-Bis{1-[(5-(5-chlorobenzimidazol-2-yl)furan-2-yl)methylene]-1H-1,2,3-triazol-4-yl}propane (**13e**).* Compound **13e** was prepared using the above described method from **8** (150 mg, 0.38 mmol) and **12e** (119.97 mg, 0.84 mmol) to obtain **13e** as brown powder (61.9 mg, 25%, m.p. = 158–161 °C). ^{1}H NMR (600 MHz, DMSO) δ 13.43–12.79 (2H, m, NH), 7.97 (2H, s, H5''), 7.70–7.45 (4H, m, H4; H7), 7.21 (4H, d, *J* = 3.2 Hz, H6, H3'), 6.79 (2H, d, *J* = 3.1 Hz, H4'), 5.73 (4H, s, CH_2), 2.67 (4H, t, *J* = 7.4 Hz, CH_2), 1.93 (2H, dt, *J* = 14.8, 7.4 Hz, CH_2). ^{13}C NMR (75 MHz, DMSO) δ 150.54, 146.92, 145.34, 144.36, 122.62, 122.02, 112.38, 112.02, 45.70, 28.69, 24.52. Anal. calcd. for $C_{31}H_{24}N_{10}Cl_2O_2$ × 2.2 H_2O (*Mr* = 679.13): C 54.83, H 4.21, N 20.62; found: C 55.06, H 4.36, N 20.48%.

*4.2.5.3. 1,3-Bis{1-[(5-(benzimidazol-2-yl)furan-2-yl)methylene]-1H-1,2,3-triazol-4-yl}propane (**13f**).* Compound **13f** was prepared using the above described method from **8** (130 mg, 0.33 mmol) and **12f** (78.42 mg, 0.72 mmol) to obtain **13f** as yellow powder (185.8 mg, 99%, m.p. = 154–156 °C). ^{1}H NMR (300 MHz, DMSO) δ 7.96 (2H, s, H5''), 7.65–7.46 (4H, m, *J* = 5.6, 3.0 Hz, H4; H7), 7.24–7.16 (6H, m, H5; H6; H3'), 6.77 (2H, d, *J* = 3.1 Hz, H4'), 5.72 (4H, s, CH_2), 2.67 (4H, t, *J* = 7.4 Hz, CH_2), 2.03–1.81 (2H, m, CH_2).^{13}C NMR (75 MHz, DMSO) δ 150.26, 146.92, 145.67, 143.01, 122.45, 122.02, 112.31, 111.50, 45.72, 28.70, 24.53. Anal. calcd. for $C_{31}H_{26}N_{10}O_2$ × 3.9 H_2O (*Mr* = 639.07): C 58.26, H 5.30, N 21.92; found: C 58.00, H 5.53, N 22.24%.

*4.2.5.4. Bis{1-[(5-(5-fluorobenzimidazol-2-yl)furan-2-yl)methylene]-1H-1,2,3-triazol-4-yl}dimethylene ether (**14d**).* Compound **14d** was prepared using the above described method from **9** (145 mg, 0.37 mmol) and **12d** (96.90 mg, 0.77 mmol) to obtain **14d** as yellow powder (187.4 mg, 84%, m.p. = 162–165 °C. ^{1}H NMR (300 MHz, DMSO) δ 8.21 (2H, s, H5''), 7.55 (2H, dd, *J* = 8.8, 4.8 Hz, H4), 7.36 (2H, dd, *J* = 9.4, 2.3 Hz, H7), 7.20 (2H, d, *J* = 3.4 Hz, H3'), 7.07 (2H, td, *J* = 9.9, 2.4 Hz, H6), 6.80 (2H, d, *J* = 3.4 Hz, H4'), 5.77 (4H, s, CH_2), 4.59 (4H, s, CH_2). ^{13}C NMR (151 MHz, DMSO) δ 159.60; 158.03 (d, J_{CF} = 235.9 Hz), 150.31, 145.18, 144.08, 124.12, 112.49, 111.94, 110.76; 110.59 (d, J_{CF} = 25.5 Hz), 62.71, 45.76. Anal. calcd. for $C_{30}H_{22}N_{10}F_2O_3 \times 0.1\ H_2O$ (*Mr* = 612.21): C 58.86, H 3.64, N 22.88; found: C 58.62, H 3.35, N 23.00%.

*4.2.5.5. Bis{1-[(5-(5-chlorobenzimidazol-2-yl)furan-2-yl)methylene]-1H-1,2,3-triazol-4-yl}dimethylene ether (**14e**).* Compound **14e** was prepared using the above described method from **9** (150 mg, 0.38 mmol) and **12e** (113.31 mg, 0.79 mmol) to obtain **14e** as yellow powder (235.1 mg, 96%, m.p. = 144–147 °C. ^{1}H NMR (300 MHz, DMSO) δ 8.20 (2H, s, H5''), 7.62–7.51 (4H, m, H4; H7), 7.24–7.19 (4H, m, H6; H3'), 6.80 (2H, d, *J* = 3.4 Hz, H4'), 5.77 (4H, s, CH_2), 4.59 (4H, s, CH_2). ^{13}C NMR (75 MHz, DMSO) δ 150.33, 145.39, 144.30, 144.09, 126.62, 124.15, 122.61, 112.52, 112.02, 62.71, 45.78. Anal. calcd. for $C_{30}H_{22}N_{10}Cl_2O_3 \times 0.4\ H_2O$ (*Mr* = 656.06): C 54.92, H 3.44, N 21.35; found: C 55.16, H 3.59, N 21.42%.

*4.2.5.6. Bis{1-[(5-(benzimidazol-2-yl)furan-2-yl)methylene]-1H-1,2,3-triazol-4-yl}dimethylene ether (**14f**).* Compound **14f** was prepared using the above described method from **9** (150 mg, 0.38 mmol) and **12f** (85.43 mg, 0.79 mmol) to obtain **14f** as yellow powder (180.2 mg, 87%, m.p. = 227–231 °C. ^{1}H NMR (300 MHz, DMSO) δ 12.94 (2H, bs, NH), 8.21 (2H, s, H5''), 7.57–7.49 (4H, m, H4; H7), 7.25– 7.13 (6H, m, H5; H6; H3'), 6.79 (2H, d, *J* = 3.4 Hz, H4'), 5.77 (4H, s, CH_2), 4.59 (4H, s, CH_2). ^{13}C NMR (75 MHz, DMSO) δ 149.97, 145.87, 144.10, 143.02, 124.15, 122.37, 112.43, 111.35, 62.73, 45.81. Anal. calcd. for $C_{30}H_{24}N_{10}O_3 \times 3.2\ H_2O$ (*Mr* = 632.04): C 57.01, H 4.88, N 22.16; found: C 56.74, H 4.96, N 22.15%.

*4.2.5.7. 1,4-Bis{[1-((5-(5-fluorobenzimidazol-2-yl)furan-2-yl)methylene)-1H-1,2,3-triazol-4-yl]methyleneoxy}benzene (**15d**).* Compound **15d** was prepared using the above described method from **10** (150 mg, 0.31 mmol) and **12d** (77.45 mg, 0.68 mmol) to obtain **15d** as light brown powder (195.4 mg, 90%, m.p. = 152–154 °C). ^{1}H NMR (300 MHz, DMSO) δ 8.29 (2H, s, H5''), 7.55 (2H, dd, *J* = 8.5, 4.7 Hz, H4), 7.35 (2H, dd, *J* = 9.2, 1.7 Hz, H7), 7.20 (2H, d, *J* = 3.1 Hz, H3'), 7.06 (2H, td, *J* = 9.3, 1.6 Hz, H6), 6.95 (4H, s, Ph), 6.82 (2H, d, *J* = 3.1 Hz, H4'), 5.80 (4H, s, CH_2), 5.06 (4H, s, CH_2). ^{13}C NMR (151 MHz, DMSO) δ 159.61; 158.05 (d, J_{CF} = 235.4 Hz), 152.31, 150.22, 145.49, 144.30, 143.35, 124.62, 115.58, 112.63, 111.80, 110.72; 110.56 (d, J_{CF} = 24.2 Hz), 61.42, 45.88. Anal. calcd. for $C_{36}H_{26}F_2N_{10}O_4 \times 1.6\ H_2O$ (*Mr* = 729.49): C 59.27, H 4.03, N 19.20; found: C 59.47, H 3.76, N 19.19%.

*4.2.5.8. 1,4-Bis{[1-((5-(5-chlorobenzimidazol-2-yl)furan-2-yl)methylene)-1H-1,2,3-triazol-4-yl]methyleneoxy}benzene (**15d**). (**15e**).* Compound **15e** was prepared using the above described method from **10** (150 mg, 0.31 mmol) and **12e** (51.62 mg, 0.68 mmol) to obtain **15e** as white powder (135.3 mg, 60%, m.p. = 160–162 °C). ^{1}H NMR (300 MHz, DMSO) δ 8.29 (2H, s, H5''), 7.66–7.52 (4H, m, H4; H/), 7.25–7.20 (4H, m, H6; H3'), 6.95 (4H. s, Ph), 6.83 (2H, d, *J* = 3.4 Hz, H4'), 5.81 (4H. s, CH_2), 5.06 (4H, s, CH_2).^{13}C NMR (75 MHz, DMSO) δ 152.29, 150.40, 145.25, 143.32, 126.74, 124.54, 122.73, 115.56, 112.63, 112.22, 61.42, 45.83. Anal. calcd. for $C_{36}H_{26}Cl_2N_{10}O_4 \times 0.9\ H_2O$ (*Mr* = 749.79): C 57.67, H 3.74, N 18.68; found: C 57.95, H 3.71, N 18.53%.

*4.2.5.9. 1,4-Bis{[1-((5-(benzimidazol-2-yl)furan-2-yl)methylene)-1H-1,2,3-triazol-4-yl]methyleneoxy}benzene (**15f**).* Compound **15f** was prepared using the above described method from **10** (150 mg, 0.31 mmol) and **12f** (73.06 mg, 0.68 mmol) to obtain **15f** as white powder (196.7 mg, 95%, m.p. = 155–157 °C). ^{1}H NMR (600 MHz, DMSO) δ 8.30 (2H, s, H5''), 7.55 (4H, s, H4; H7), 7.21–7.18 (6H, m, H6; H5; H3'), 6.95 (4H, s, CH_2), 6.81 (2H, d, *J* = 3.0 Hz, H4'), 5.80 (4H. s, CH_2), 5.06 (4H, s, CH_2).^{13}C NMR (75 MHz, DMSO) δ 152.30, 149.96, 145.89, 143.33, 124.54, 122.41, 115.58, 112.52, 111.40, 61.44, 45.87. Anal. calcd. for $C_{36}H_{28}Cl_2N_{10}O_4 \times 3.1\ H_2O$ (*Mr* = 720.53): C 60.01, H 4.78, N 19.43; found: C 59.86, H 4.61, N 19.38%.

*4.2.5.10. 4,4'-Bis{[1-((5-(5-fluorobenzimidazol-2-yl)furan-2-yl)methylene)-1H-1,2,3-triazol-4-yl]methylenoxy}-1,1'-biphenyl (**16d**).* Compound **16d** was prepared using the above described method from **11** (150 mg, 0.26 mmol) and **12d** (67.03 mg, 0.52 mmol) to obtain **16d** as light brown powder (120.5 mg, 53%, m.p. = 175–179 °C). ^{1}H NMR (300 MHz, DMSO) δ 13.06 (2H, s, NH), 8.35 (2H, s, H5''), 7.65–7.59 (2H, m, H4), 7.50 (4H, d, *J* = 8.6 Hz, Ph), 7.41 (2H, d, *J* = 9.9 Hz, H7), 7.28 (2H, dd, *J* = 8.6, 3.0 Hz, H6), 7.21–7.17 (2H, m, H3'), 7.07 (4H, d, *J* = 8.6 Hz, Ph), 6.82 (2H, s, H4'), 5.81 (4H, s, CH_2), 5.18 (4H, s, CH_2). ^{13}C NMR (75 MHz, DMSO) δ 157.03, 153.85, 149.84, 145.54, 143.06, 132.49, 131.27, 128.43, 127.01, 124.28, 115.03, 112.24, 111.32, 61.10, 45.75. Anal. calcd. for $C_{42}H_{30}F_2N_{10}O_4 \times 5.1\ H_2O$ (*Mr* = 868.64): C 58.07, H 4.66, N 16.12; found: C 57.85, H 4.64, N 16.26%.

*4.2.5.11. 4,4'-Bis{[1-((5-(5-chlorobenzimidazol-2-yl)furan-2-yl)methylene)-1H-1,2,3-triazol-4-yl]methyleneoxy}-1,1'-biphenyl (**16e**).* Compound **16e** was prepared using the above described method from **11** (160 mg, 0.28 mmol) and **12e** (88.91 mg, 0.62 mmol) to obtain **16e** as white powder (120.5 mg, 53%, m.p. = 173–176 °C). ^{1}H NMR (300 MHz, DMSO) δ 13.12 (2H, d, *J* = 14.5 Hz, NH), 8.35 (2H, s, H5''), 7.66–7.60 (2H, m, H4), 7.57–7.44 (6H, m, H7; Ph), 7.29–7.18 (4H, m, H6; H3'), 7.07 (4H, d, *J* = 8.4 Hz, Ph), 6.83 (2H, d, *J* = 3.0 Hz, H4'), 5.82 (4H, s, CH_2), 5.18 (4H, s, CH_2). ^{13}C NMR (151 MHz, DMSO) δ 157.15, 150.34, 145.52, 144.55, 143.18, 142.42, 132.55, 127.25, 127.11, 126.30, 124.78, 122.97, 120.14, 118.24, 115.10, 112.68, 111.17, 61.03, 45.89. Anal. calcd. for $C_{42}H_{30}Cl_2N_{10}O_4 \times 4.3\ H_2O$ (*Mr* = 887.13): C 56.86, H 4.38, N 15.79; found: C 56.66, H 4.64, N 15.56%.

*4.2.5.12. 4,4'-Bis{[1-((5-(benzimidazol-2-yl)furan-2-yl)methylene)-1H-1,2,3-triazol-4-yl]methyleneoxy}-1,1'-biphenyl (**16f**).* Compound **16f** was prepared using the above described method from **11** (100 mg, 0.18 mmol) and **12ef** (42.14 mg, 0.39 mmol) to obtain **16f** as light brown powder (120.14 mg, 90%, m.p. = 171–173 °C). ^{1}H NMR (600 MHz, DMSO) δ 8.37 (2H, s, H5''), 7.59–7.56 (4H, m, H4; H7), 7.49 (4H, d, *J* = 8.6 Hz, Ph), 7.23–7.21 (6H, m, H5; H6; H3'), 7.07 (4H, d, *J* = 8.7 Hz, Ph), 6.84 (2H, d, *J* = 3.2 Hz, H4'), 5.82 (4H, s, CH_2), 5.18 (4H, s, CH_2). ^{13}C NMR (75 MHz, DMSO) δ 157.13, 150.21, 145.45, 143.18, 136.67, 132.54, 127.21, 124.72, 122.69, 115.09, 112.64, 112.48,

111.89, 61.05, 45.89. Anal. calcd. for $C_{42}H_{32}N_{10}O_4 \times 3.3\ H_2O$ (*Mr* = 800.23): C 63.04, H 4.86, N 17.50; found: C 62.85, H 4.64, N 17.62%.

4.3. *Spectroscopic experiments*

4.3.1. Polynucleotides

Poly A–poly U and calf thymus DNA (*ct*DNA) were purchased from Sigma-Aldrich. Polynucleotides were dissolved in PBS buffer, I = 0.05 mol dm^{-3}, pH 7.0. The calf thymus *ct*DNA was additionally sonicated and filtered through a 0.45 mm filter. The polynucleotide concentration was spectroscopically determined as the concentration of nucleobases [50].

4.3.2. UV-Visible Spectroscopy

All UV-visible absorbance measurements were conducted on a Perkin Elmer Lambda 25 spectrophotometer. A quartz cell with a 1 cm path length was used for all absorbance studies. Compound stock solutions were 1 mM. The DNA/RNA at increasing ratios was then titrated into the compound buffer solution (0.6-1.5·10^{-5} mol dm^{-3}) and the corresponding absorption spectra were recorded under the same conditions. All data were graphed and analyzed using Origin software 9.0. The stability constants (Ks) and [bound compound]/[polynucleotide phosphate] ratio (n) were calculated according to the Scatchard equation [51,52]. Values for Ks and n are given in Table 1; all have satisfying correlation coefficients (0.99).

4.3.3. Thermal Melting (T_m)

Tm experiments were conducted with a Perkin Elmer Lambda 25 spectrophotometer in 1 cm quartz cuvettes. The absorbance of the DNA-compound complex was monitored at 260 nm as a function of temperature. The absorbance of the ligands was subtracted from every curve, and the absorbance scale was normalized. The ΔT_m values were calculated by subtracting Tm of the free nucleic acid from Tm of the complex. Every reported ΔT_m value was the average of at least two measurements. The error of ΔT_m is ±0.5 °C. All data was graphed and analyzed using Origin software 9.0.

4.3.4. Circular Dichroism(CD)

The CD spectra of DNA/RNA (concentration in cuvette $2 \cdot 10^{-5}$ M) were recorded with a JASCO J-800 spectrometer at different ratios r = 0.1, 0.3, 0.5, 0.7 (r = [compound]/ [polynucleotide]) at 25°C in aqueous buffer solution (pH = 7, PBS, I = 0.05 mol dm^{-3}). Titrations were carried out by addition of aliquots of 1 mM stock solutions of the relevant compound (at increasing ratios) to the buffered polynucleotide (DNA/RNA) solution in a 1 cm quartz cuvette and scanned over a wavelength range 220-450 nm. All data were graphed and analyzed using Origin software 9.0.

4.4. Antitrypanosomal screening

Bloodstream form *T. brucei* (strain 221) were grown in modified Iscove's medium, as described [53] and growth inhibition assays were performed using 96-well microtiter plates. The compound concentrations that inhibited growth by 50% (IC_{50}) and 90% (IC_{90}) were determined. Parasites were initially sub-cultured at 2.5×10^4 mL^{-1}, compounds were added at range of concentrations, and the plates incubated at 37 °C. Resazurin was added after 48 h, the plates incubated for a further 16 hours, and then read in a Spectramax plate reader. The data were analysed using GraphPad Prism. Each drug concentration was tested in triplicate.

For cytotoxicity assays, L6 cells (a rat myoblast line) were seeded into 96-well microtiter plates at 1 x 10^4 mL^{-1} in 200 µL of growth medium, and different compound concentrations were added. The plates were then incubated for 6 days at 37 °C and 20 µL resazurin added to each well. After further 8 hours incubation, the fluorescence was determined using a Spectramax plate reader, as outlined above.

4.5. In silico molecular modelling

Interactions between **15c** and DNA were studied using two different nucleotides: *Drew*-Dickerson dodecamer (12 bp DNA) $d[(CGCGAATTCGCG)]_2$ encoded in Protein Data Bank (PDB) [54] as 1BNA [55] and the 14 bp B-DNA $d[(CTACCGATAAGCAG)]_2$ extracted from the crystalographically determined structure of the complex between DNA and RNA polymerase (pdb: 5XOG) [56]. The ligand was

accommodated into the ds-DNA minor groove visually by using the program InsightII. The AMBER ff14SB force field [57] and the general AMBER force field gaff [58] were used to parameterize the ligand–DNA complexes. Geometry optimization and molecular dynamics (MD) simulations were accomplished by using the AMBER16 program package [59]. The simulation was accomplished by using periodic boundary conditions (PBC). The particle mesh Ewald (PME) method was used for calculation of the long-range electrostatic interactions, and in the direct space the pairwise interactions were calculated within the cut-off distance of 10 Å. Each of the complexes were placed in the center of a octahedron filled with TIP3P-type water molecules, and Cl^- and Na^+ ions were added to neutralize the systems. The solvated complexes were geometry optimized by using steepest descent and conjugate gradient methods, 1500 steps of each, and equilibrated for 1.5 ns. During the first stage of equilibration (30 ps) the temperature was linearly increased from 0 to 300 K and the volume was held constant. In the second stage temperature and pressure were held fixed (300 K and 1 atm, respectively) and the solution density was optimized. The equilibrated **15c**–DNA complexes were subjected to productive molecular dynamics simulation using NPT condition and the time step of 2 fs, except SHAKE (constrains bonds involving hydrogen atoms) [60] no restraints were used. In the case of the **15c** complex with 14 bp 70 ns and in the case of the complex with dodecamer 160 ns of the productive MD simulations was accomplished. The temperature was held constant using Langevin thermostat [61] with a collision frequency of 1 ps^{-1}. Pressure was regulated by a Berendsen barostat [62].

Declaration of interest

Declaration of interest: none.

Acknowledgment

We greatly appreciate the financial support of the Croatian Science Foundation (project No. IP-2018-01-4682).

References

[1] D.H. Molyneux, Neglected tropical diseases: now more than just 'other diseases'–the post-2015 agenda. Int. Health. 6 (2014) 172–180. doi: 10.1093/inthealth/ihu037.

[2] Centers for Disease Control and Prevention, Neglected Tropical Diseases. http:/www.cdc.gov/globalhealth/ntd/, 2016 (accesed 15 June 2016)

[3] M. Njoroge, N.M. Njuguna, P. Mutai, D.S. Ongarora, P.W. Smith, K. Chibale, Recent approaches to chemical discovery and development against malaria and the neglected tropical diseases human African trypanosomiasis and schistosomiasis. Chem. Rev. 114 (2014) 11138–11163. doi: 10.1021/cr500098f.

[4] I. Sola, A. Artigas, M.C. Taylor, F.J. Pérez-Areales, E. Viayna, M.V. Clos, B. Pérez, C.W. Wright, J.M. Kelly, D. Muñoz-Torrero, Synthesis and biological evaluation of N-cyanoalkyl-, N-aminoalkyl-, and N-guanidinoalkyl-substituted 4-aminoquinoline derivatives as potent, selective, brain permeable antitrypanosomal agents. Bioorg. Med. Chem. 24 (2016) 5162–5171. doi: 10.1016/j.bmc.2016.08.036.

[5] M.P. Barrett, C.G. Gemmell, C.J. Suckling, Minor groove binders as anti-infective agents. Pharmacol. Ther. 139 (2013) 12–23. doi: 10.1016/j.pharmthera.2013.03.002.

[6] P.G. Bray, M.P. Barrett, S.A. Ward, H.P. de Koning, Pentamidine uptake and resistance in pathogenic protozoa: past, present and future. Trends Parasitol. 19 (2003) 232–239. doi: 10.1016/S1471-4922(03)00069-2.

[7] S. Kuriakose, J.E. Uzonna, Diminazene aceturate (Berenil), a new use for an old compound. Int. Immunopharmacol. 21 (2014) 342–345. doi: 10.1016/j.intimp.2014.05.027.

[8] B. Bouteille, O. Oukem, S. Bisser, M. Dumas, Treatment perspectives for human African trypanosomiasis. Fundam. Clin. Pharmacol. 17 (2003) 171–181. doi: 10.1046/j.1472-8206.2003.00167.x.

[9] R.P. Bakshi, T.A. Shapiro, DNA topoisomerases as targets for antiprotozoal therapy. Mini Rev. Med. Chem. 3 (2003) 597–608. doi: 10.2174/1389557033487863.

[10] R.R. Tidwell, D.W. Boykin, Dicationic DNA minor groove binders as antimicrobial agents, in M. Demeunynck, C. Bailly, W.D. Wilson, (Eds.), DNA and RNA binders: From small molecules to drugs, WILEY-VCH; Weinheim, 2003. Vol. 2, pp. 414–460.

[11] V. Delespaux, H.P. de Koning, Drugs and drug resistance in African trypanosomiasis. Drug Resist. Updat. 10 (2007) 30–50. doi: 10.1016/j.drup.2007.02.004.

[12] W.D. Wilson, F.A. Tanious, A. Mathis, D. Tevis, J.E. Hall, D.W. Boykin, Antiparasitic compounds that target DNA. Biochimie. 90 (2008) 999–1014. doi: 10.1016/j.biochi.2008.02.017.

[13] J. Mosqueda, A. Olvera-Ramirez, G. Aguilar-Tipacamu, G.J. Canto, Current advances in detection and treatment of babesiosis. Curr. Med. Chem. 19 (2012) 1504–1518. doi: 10.2174/092986712799828355.

[14] J.H. Ansede, M. Anbazhagan, R. Brun, J.D. Easterbrook, J.E. Hall, D.W. Boykin, O-alkoxyamidine prodrugs of furamidine: in vitro transport and microsomal metabolism as indicators of in vivo efficacy in a mouse model of Trypanosoma brucei rhodesiense infection. J. Med. Chem. 47 (2004) 4335–4338. doi: 10.1021/jm030604o.

[15] M.F. Paine, M. Z. Wang, C.N. Generaux, D.W. Boykin, W.D. Wilson, H.P. De Koning, C.A. Olson, G. Pohlig, C.Burr, R. Brun, G.A. Murilla, J.K. Thuita, M.P. Barrett, R.R. Tidwell, Diamidines for human African trypanosomiasis. Curr. Opin. Invest. Drugs. 11 (2010) 876–883.

[16] W.D. Wilson, B. Nguyen, F.A. Tanious, A. Mathis, J.E. Hall, C.E. Stephens, D.W. Boykin, Dications that target the DNA minor groove: compound design and preparation, DNA interactions, cellular distribution and biological activity. Curr. Med. Chem. Anticancer. Agents. 5 (2005) 389–408. doi: 10.2174/1568011054222319.

[17] M.N.C. Soeiro, K. Werbovetz, D.W. Boykin, W.D. Wilson, M.Z. Wang, A. Hemphill, Novel amidines and analogues as promising agents against intracellular parasites: a systematic review. Parasitol. 140 (2013) 929–951. doi: 10.1017/S0031182013000292.

[18] G. Yang, G. Choi, J.H. No, Antileishmanial mechanism of diamidines involves targeting kinetoplasts. Antimicrob. Agents Chemother. 60 (2016) 6828–6836. doi: 10.1128/AAC.01129-16.

[19] A.M. Mathis, A.S. Bridges, M.A. Ismail, A. Kumar, I. Francesconi, M. Anbazhagan, Q. Hu, F.A. Tanious, T. Wenzler, J. Saulter, W.D. Wilson, R. Brun, D.W. Boykin, R.T. Tidwell, J.E. Hall, Diphenyl furans and aza analogs: effects of structural modification on in vitro activity, DNA binding, and accumulation and distribution in trypanosomes. Antimicrob. Agents Chemother. 51 (2007) 2801–2810. doi. 10.1128/AAC.00005-07.

[20] H.P. de Koning, Ever-increasing complexities of diamidine and arsenical crossresistance in African trypanosomes. Trends Parasitol. 24 (2008) 345–349. doi: 10.1016/j.pt.2008.04.006.

[21] C.P. Ward, P.E. Wong, R.J. Burchmore, H.P. de Koning, M.P. Barrett, Trypanocidal furamidine analogues: influence of pyridine nitrogens on trypanocidal activity, transport kinetics, and resistance patterns. Antimicrob. Agents Chemother. 55 (2011) 2352–2361. doi: 10.1128/AAC.01551-10.

[22] S. Melchor, D. de la Torre, C. Vázquez, Z. González-Chávez, L. Yépez-Mulia, R. Nieto-Meneses, R. Jasso, E. Saavedra, F. Hernández-Luis, Synthesis and biological evaluation of 2-methyl-1H-benzimidazole-5-carbohydrazides derivatives as modifiers of redox homeostasis of Trypanosoma cruzi. Bioorg. Med. Chem. Lett. 27 (2017) 3403–3407. doi: 10.1016/j.bmcl.2017.06.013

[23] I. Pauli, L.G. Ferreira, M.L. de Souza, G. Oliva, R.S. Ferreira, M.A. Dessoy, B.W. Slafer, L.C. Dias, A.D. Andricopulo, Molecular modeling and structure–activity relationships for a series of benzimidazole derivatives as cruzain inhibitors. Future Med. Chem. 9 (2017) 641–657. doi: 10.4155/fmc-2016-0236.

[24] J.M. Velázquez-López, A. Hernández-Campos, L. Yépez-Mulia, A. Téllez-Valencia, P. Flores-Carrillo, R. Nieto-Meneses, R. Castillo, Synthesis and trypanocidal activity of novel benzimidazole derivatives. Bioorg. Med. Chem. Lett. 26 (2016) 4377–4381. doi: 10.1016/j.bmcl.2015.08.018.

[25] M. Boiani, L. Boiani, A. Merlino, P. Hernández, A. Chidichimo, J.J. Cazzulo, H. Cerecetto, M. González, Second generation of 2H-benzimidazole 1, 3-dioxide

derivatives as anti-trypanosomatid agents: Synthesis, biological evaluation, and mode of action studies. Eur. J. Med. Chem. 44 (2009) 4426–4433. doi: 10.1016/j.ejmech.2009.06.014.

[26] C. Karaaslan, M. Kaiser, R. Brun, H. Göker, Synthesis and potent antiprotozoal activity of mono/di amidino 2-anilinobenzimidazoles versus Plasmodium falciparum and Trypanosoma brucei rhodesiense. Bioorg. Med. Chem. 24 (2016) 4038–4044. doi: 10.1016/j.bmc.2016.06.047.

[27] A.A. Farahat, C. Bennett-Vaughn, E.M. Mineva, A. Kumar, T. Wenzler, R. Brun, Y. Liu, W.D. Wilson, D.W. Boykin, Synthesis, DNA binding and antitrypanosomal activity of benzimidazole analogues of DAPI. Bioorg. Med. Chem. Lett. 26 (2016) 5907–5910. doi: 10.1016/j.bmcl.2016.11.006.

[28] M.A. Ismail, R. Brun, T. Wenzler, F.A. Tanious, W.D. Wilson, D.W. Boykin, Dicationic biphenyl benzimidazole derivatives as antiprotozoal agents. Bioorg. Med. Chem. 12 (2004) 5405–5413. doi: 10.1016/j.bmc.2004.07.056.

[29] M.A. Ismail, A. Batista-Parra, Y. Miao, W.D. Wilson, T. Wenzler, R. Brun, D.W. Boykin, Dicationic near-linear biphenyl benzimidazole derivatives as DNA-targeted antiprotozoal agents. Bioorg. Med. Chem. 13 (2005) 6718–6726. doi: 10.1016/j.bmc.2005.07.024.

[30] S.A. Bakunov, S.M. Bakunova, T. Wenzler, M. Ghebru, K.A. Werbovetz, R. Brun, R.R. Tidwell, Synthesis and antiprotozoal activity of cationic 1,4-diphenyl-1H-1,2,3-triazoles. J. Med. Chem. 53 (2009) 254–272. doi: 10.1021/jm901178d.

[31] L. Krstulović, I. Stolić, M. Jukić, T. Opačak-Bernardi, K. Starčević, M. Bajić, L. Glavaš-Obrovac, New quinoline-arylamidine hybrids: Synthesis, DNA/RNA binding and antitumor activity. Eur. J. Med. Chem. 137 (2017) 196–210. doi: 10.1016/j.ejmech.2017.05.054.

[32] I. Stolić, H.Č. Paljetak, M. Perić, M. Matijašić, V. Stepanić, D. Verbanac, M. Bajić, Synthesis and structure–activity relationship of amidine derivatives of 3,4-ethylenedioxythiophene as novel antibacterial agents. Eur. J. Med. Chem. 90 (2015) 68–81. doi: 10.1016/j.ejmech.2014.11.003.

[33] A. Bistrović, L. Krstulović, I. Stolić, D. Drenjančević, J. Talapko, J. M. Kelly, M. Bajić, S. Raić-Malić, Synthesis, DNA/RNA-binding, antibacterial and antiprotozoal activities of novel 5-amidinobenzimidazoles. J. Enzyme Inhib. Med. Chem. 33 (2018) 271–285. doi: 10.1080/14756366.2017.1414807.

[34] R.M.B.M. Girard, M. Crispim, I. Stolić, F.S. Damasceno, M.S. da Silva, E.M. Furusho Pral, M.C. Elias, M. Bajić, A.M. Silber, An aromatic diamidine that targets kinetoplast DNA, impairs the cell cycle in Trypanosoma cruzi, and diminishes Trypomastigote release from infected mammalian cell. Antimicrob. Agents Chemother. 60 (2016) 5867–5877. doi: 10.1128/AAC.01595-15.

[35] M. Mascal, E.B. Nikitin, Dramatic advancements in the saccharide to 5-(chloromethyl) furfural conversion reaction. Chem. Sus. Chem. 2 (2009) 859–861 doi: 10.002/cssc.200900136.

[36] W. Gao, Y. Li, Z. Xiang, K. Chen, R. Yang, D.S. Argyropoulos, Efficient one-pot synthesis of 5-chloromethylfurfural (CMF) from carbohydrates in mild biphasic systems. Molecules 18 (2013) 7675–7685. doi: 10.3390/molecules18077675.

[37] M. Hranjec, K. Starcevic, B. Zamola, S. Mutak, M. Derek, G. Karminski-Zamola, New amidino-benzimidazolyl derivatives of tylosin and desmycosin. J. Antibiot. 55 (2002) 308–314. doi: 10.7164/antibiotics.55.308.

[38] S.U. Rehman, T. Sarwar, M.A. Husain, H.M. Ishqi, M. Tabish, Studying non-covalent drug–DNA interactions. Arch. Biochem. Biophys. 576 (2015) 49–60. doi: 10.1016/j.abb.2015.03.024.

[39] M. Ganeshpandian, S. Ramakrishnan, M. Palaniandavar, E. Suresh, A. Riyasdeen, M.A. Akbarsha, Mixed ligand copper (II) complexes of 2,9-dimethyl-1,10-phenanthroline: Tridentate 3N primary ligands determine DNA binding and cleavage and cytotoxicity. J. Inorg. Biochem. 140 (2014) 202–212. doi: 10.1016/j.jinorgbio.2014.07.021.

[40] N. Shahabadi, S. Hadidi, Spectroscopic studies on the interaction of calf thymus DNA with the drug levetiracetam. Spectrochim. Acta Mol. Biomol. Spectrosc. 96 (2012) 278–283. doi: 10.1016/j.saa.2012.05.045.

[41] W.D. Wilson, F.A. Tanious, M. Fernandez-Saiz, C.T. Rigl, Evaluation of drug-nucleic acid interactions by thermal melting curves. Method. Mol. Biol. 90 (1997) 219–240. doi: 10.1385/0-89603-447-X:219.

[42] S. Alnabulsi, E. Santina, I. Russo, B. Hussein, M. Kadirvel, A. Chadwick, E.V. Bichenkova, R.A. Bryce, K. Nolan, C. Demonacos, I.J. Stratford, Non-symmetrical furan-amidines as novel leads for the treatment of cancer and malaria. Eur. J. Med. Chem. 111 (2016) 33–45. doi: 10.1016/j.ejmech.2016.01.022

[43] Y. Liu, A. Kumar, D.W. Boykin, W.D.Wilson, Sequence and length dependent thermodynamic differences in heterocyclic diamidine interactions at AT base pairs in the DNA minor groove. Biophys. Chem. 131 (2007) 1–14. doi: 10.1016/j.bpc.2007.08.007.

[44] P. O'Sullivan, I. Rozas, Understanding the Guanidine-Like Cationic Moiety for Optimal Binding into the DNA Minor Groove. Chem. Med. Chem, 9 (2014) 2065–2073. doi: 10.1002/cmdc.201402264.

[45] D. Havrylyuk, B. Zimenkovsky, O. Karpenko, P. Grellier, R. Lesyk, Synthesis of pyrazoline–thiazolidinone hybrids with trypanocidal activity. Eur. J. Med. Chem. 85 (2014) 245–254. doi: 10.1016/j.ejmech.2014.07.103.

[46] L.M. Tumir, I. Crnolatac, T. Deligeorgiev, A. Vasilev, S. Kaloyanova, M. Grabar Branilović, S. Tomić, I. Piantanida, Kinetic differentiation between homo- and alternating AT-DNA by sterically restricted phosphonium dyes. Chem. Eur. J. 18 (2012) 3859–3864. doi: 10.1002/chem.201102968.

[47] R. Palchaudhuri, P.J. Hergenrother, DNA as a target for anticancer compounds: methods to determine the mode of binding and the mechanism of action. Curr. Opin. Biotechnol. 18 (20079 497–503. doi: 10.1016/j.copbio.2007.09.006.

[48] A. Anand, R.J. Naik, H.M. Revankar, M.V. Kulkarni, S.R. Dixit, S.D. Joshi, A click chemistry approach for the synthesis of mono and bis aryloxy linked coumarinyl triazoles as anti-tubercular agents. Eur. J. Med. Chem. 105 (2015) 194–207. doi: 10.1016/j.ejmech.2015.10.019.

[49] Q. Li, K. Han, J. Li, X. Jia, C. Li, Synthesis of dendrimer-functionalized pillar [5] arenes and their self-assembly to dimeric and trimeric

complexes. Tetrahedron Lett. 56 (2015) 3826–3829. doi: 10.1016/j.tetlet.2015.04.078.

[50] I. Stolić, K. Mišković, A. Magdaleno, A.M. Silber, I. Piantanida, M. Bajić, L. Glavaš-Obrovac, Effect of 3, 4-ethylenedioxy-extension of thiophene core on the DNA/RNA binding properties and biological activity of bis benzimidazole amidines. Bioorg. Med. Chem. 17 (2009) 2544–2554. doi: 10.1016/j.bmc.2009.01.071.

[51] G. Scatchard, The attractions of proteins for small molecules and ions. Ann. N. Y. Acad. Sci. 51 (1949) 660–672. doi: 10.1111/j.1749-6632.1949.tb27297.x.

[52] J.D. McGhee, P.H. von Hippel, Theoretical aspects of DNA-protein interactions: co-operative and non-co-operative binding of large ligands to a one-dimensional homogeneous lattice. J. Mol. Biol. 86 (1974) 469–489. doi: 10.1016/0022-2836(74)90031-X.

[53] M.C. Taylor, M.D. Lewis, A. Fortes Francisco, S.R. Wilkinson, J.M. Kelly, The *Trypanosoma cruzi* vitamin C dependent peroxidase confers protection against oxidative stress but is not a determinant of virulence. PLoS Negl. Trop. Dis. 9 (4) (2015) e0003707. doi: 10.1371/journal.pntd.0003707.

[54] H.M. Berman, J. Westbrook, Z. Feng, G. Gilliland, T.N. Bhat, H. Weissig, I.N. Shindyalov, P.E. Bourne, The Protein Dana Bank, Nucleic Acid Res. 28 (2000) 235–242. doi: 10.1093/nar/28.1.235.

[55] H.R. Drew, R.M. Wing, T. Takano, C. Broka, S. Tanaka, K. Itakura, R.E. Dickerson, Structure of a B-DNA dodecamer: conformation and dynamics. Proc. Natl. Acad. Sci. USA. 78 (1981) 2179–2183. doi: 10.1073/pnas.78.4.2179.

[56] H. Ehara, T. Yokoyama, H. Shigematsu, S. Yokoyama, M. Shirouzu, S.I. Sekine, Structure of the complete elongation complex of RNA polymerase II with basal factors. Science 357 (2017) 921–924. doi: 10.1126/science.aan8552.

[57] J. Maier, C. Martinez, K. Kasavajhala, L. Wickstrom, K. Hauser, C. Simmerling, ff14SB: improving the accuracy of protein side chain and backbone parameters from ff99SB. J. Chem. Theory Comput. 11 (2015) 3696–3713. doi: 10.1021/acs.jctc.5b00255.

[58] J. Wang, R.M. Wolf, J. Caldwell, P.A. Kollman, D.A. Case, Development and testing of a general amber force field. J. Comput. Chem. 25 (2004) 1157–1174. doi: 10.1002/jcc.20035.

[59] D.A. Case, R.M. Betz, D.S. Cerutti, T.E. Cheatham, T. Darden, R.E. Duke, T.J. Giese, H. Gohlke, A.W. Goetz, N. Homeyer, S. Izadi, P. Janowski, J. Kaus, A. Kovalenko, T.S. Lee, S. LeGrand, P. Li, C. Lin, T. Luchko, R. Luo, B. Madej, D. Mermelstein, K.M. Merz, G. Monard, H. Nguyen, H.T. Nguyen, I. Omelyan, A. Onufriev, D.R. Roe, A. Roitberg, C. Sagui, C. Simmerling, W.M. Botello-Smith, J. Swails, R.C. Walker, J. Wang, R.M. Wolf, X. Wu, L. Xiao and P.A. Kollman, AMBER16, 2016, University of California, San Francisco.

[60] J.P. Ryckaert, G. Ciccotti, H.J.C. Berendsen, Numerical integration of the cartesian equations of motion of a system with constraints: molecular dynamics of n-alkanes. J. Comput. Phys. 23(1997) 327–341. doi: 10.1016/0021-9991(77)90098-5.

[61] R.J. Loncharich, B.R. Brooks; R.W. Pastor, Langevin dynamics of peptides: The frictional dependence of isomerization rates of N-acetylalanyl-N′-methylamide. Biopolymers 32 (1992) 523–535. doi: 10.1002/bip.360320508.

[62] H.J.C. Berendsen, J.P.M. Postma, W.F. van Gunsteren, A. DiNola, J.R. Haak, Molecular dynamics with coupling to an external bath J. Chem. Phys. 81 (1984) 3684–3690. doi: 10.1063/1.448118.